Soil nutrient competitive traits of plants, microbes, and mineral surfaces explain nutrient acquisition in tropical experimental manipulations

Qing Zhu[1*], William J. Riley[1], Jinyun Tang[1], Charles D. Koven[1]

[1] Climate Sciences Department, Earth Sciences Division, Lawrence Berkeley National Laboratory, Berkeley, CA 94720

[*] Correspondence to: Q. Zhu (qzhu@lbl.gov)

Abstract

Soil is a complex system where biotic (*e.g.*, plant roots, micro-organisms) and abiotic (*e.g.*, mineral surfaces) consumers compete for resources necessary for life (*e.g.*, nitrogen, phosphorus). This competition is ecologically significant, since it regulates the dynamics of soil nutrients and controls aboveground plant productivity. Here we develop, calibrate, and test a nutrient competition model that accounts for multiple soil nutrients interacting with multiple biotic and abiotic consumers. As applied here for tropical forests, the Nutrient COMpetition model (N-COM) includes three primary soil nutrients (NH_4^+, NO_3^-, and PO_x (representing the sum of PO_4^{3-}, HPO_4^{2-}, and $H_2PO_4^-$)) and five potential competitors (plant roots, decomposing microbes, nitrifiers, denitrifiers, and mineral surfaces). The competition is formulated with a quasi-steady-state chemical equilibrium approximation to account for substrate (multiple substrates share one consumer) and consumer (multiple consumers compete for one substrate) effects. N-COM successfully reproduced observed soil heterotrophic respiration, N_2O emissions, free phosphorus, sorbed phosphorus, and NH_4^+ pools at a tropical forest site (Tapajos). The overall model uncertainty was moderately well constrained. Our sensitivity analysis revealed that soil nutrient competition was primarily regulated by consumer-substrate

affinity rather than environmental factors such as soil temperature or soil moisture. Our results also imply that under strong nutrient limitation, relative competitiveness depends strongly on the competitor functional traits (affinity and nutrient carrier enzyme abundance). We then applied the N-COM model to analyze field nitrogen and phosphorus perturbation experiments in two tropical forest sites (in Hawaii and Puerto Rico) not used in model development or calibration. Under soil inorganic nitrogen and phosphorus elevated conditions, the model accurately replicated the experimentally observed competition among nutrient consumers. Although we used as many observations as we could obtain, more nutrient addition experiments in tropical systems would greatly benefit model testing and calibration. In summary, the N-COM model provides an ecologically consistent representation of nutrient competition appropriate for land BGC models integrated in Earth System Models.

1 Introduction

Atmospheric CO_2 concentrations have risen sharply since the pre-industrial era, primarily due to anthropogenic fossil fuel combustion and land use and land cover change [*Houghton*, 2003; *Le Quéré et al.*, 2013; *Marland et al.*, 2003]. Terrestrial ecosystems mitigate the increasing atmospheric CO_2 trend by absorbing roughly a quarter of anthropogenic CO_2 emissions [*Le Quéré et al.*, 2009]. However, it is still an open question whether the terrestrial CO_2 sink can be sustained [*Sokolov et al.*, 2008; *Zaehle et al.*, 2010], given that plant productivity is generally limited by soil nutrients [*Elser et al.*, 2007; *LeBauer and Treseder*, 2008; *Vitousek and Howarth*, 1991] and soil nutrients could be quickly depleted through biogeochemical [*Chauhan et al.*, 1981; *Nordin et al.*, 2001; *Shen et al.*, 2011] and hydrological [*Dise and Wright*, 1995; *Perakis and Hedin*, 2002] processes. Therefore, a holistic representation of soil nutrient dynamics is critically important to model the responses of terrestrial ecosystem CO_2 uptake to climate change.

Until recently, land models integrated in Earth System Models (ESMs) have largely ignored the close coupling between soil nutrient dynamics and the carbon cycle, although the impacts of soil nutrients (primarily Nitrogen and Phosphorus) regulating carbon-climate feedback are clearly required in ecosystem biogeochemistry and land models [*Zaehle and Dalmonech*, 2011; *Zhang et al.*, 2011]. For example, none of the land models in C^4MIP (Coupled Climate Carbon Cycle Model Intercomparison Project phase 4) had coupled Carbon and Nitrogen dynamics [*Friedlingstein et al.*, 2006]. The current generation of CMIP5 [*Anav et al.*, 2013] models used for the recent IPCC (Intergovernmental Panel on Climate Change) assessment had only two members (CLM4CN: *Thornton et al.* [2007]; and BNU-ESM: [*Ji et al.*, 2014]) that considered

59 nitrogen regulation of terrestrial carbon dynamics. However, as discussed below, several
60 recent studies have shown that these models had large biases in most of the individual
61 processes important for simulating nutrient dynamics. We therefore believe that, at the
62 global scale, no credible representation of nutrient constraints on terrestrial carbon
63 cycling yet exists in ESMs.
64 Further, none of the CMIP5 ESMs included a phosphorus cycle, which is likely
65 important for tropical forest carbon budgets [*Vitousek and Sanford*, 1986]. The recent
66 IPCC report highlights the importance of nitrogen and phosphorus availability on land
67 carbon storage, even though the phosphorus limitation effect is uncertain [*Stocker et al.*,
68 2013]. Since the next generation of ESMs participating in the CMIP6 synthesis will
69 continue to focus on the impacts of a changing climate on terrestrial CO_2 and abiotic
70 exchanges with the atmosphere [*Provides*, 2014], developing ecologically realistic and
71 observationally-constrained representations of soil nutrient dynamics and carbon-nutrient
72 interactions in ESMs is critical.
73 The importance of nutrient limitations in terrestrial ecosystems has been widely
74 demonstrated by nitrogen and phosphorus fertilization experiments [*Elser et al.*, 2007].
75 For instance, plant Net Primary Production (NPP) is enhanced in plots with nutrient
76 addition [*LeBauer and Treseder*, 2008]. Similarly, plant growth can be stimulated due to
77 atmospheric nitrogen deposition [*Matson et al.*, 2002]. Boreal forests are strongly limited
78 by nitrogen availability [*Vitousek and Howarth*, 1991], because low temperatures reduce
79 nitrogen mineralization [*Bonan and Cleve*, 1992] and N_2 fixation [*DeLuca et al.*, 2008;
80 *DeLuca et al.*, 2002]. In contrast, tropical forests are often phosphorus limited [*Vitousek*
81 *et al.*, 2010], since tropical soils are old and phosphorus derived from parent material

82 weathering has been depleted through long-term pedogenesis processes [*Vitousek and*
83 *Farrington*, 1997; *Walker and Syers*, 1976]. In natural ecosystems without external
84 nutrients inputs (*e.g.*, N deposition), soil nitrogen or phosphorus (or both) are likely
85 insufficient to satisfy both plant and microorganism demands [*Vitousek and Farrington*,
86 1997]. Plants have to compete with microorganisms and mineral surfaces [*Kaye and*
87 *Hart*, 1997; *Schimel et al.*, 1989] to obtain sufficient nutrients to sustain their biological
88 processes (*e.g.*, photosynthesis, respiration). Therefore, it is critical to improve the
89 representation of nutrient competition to accurately model how terrestrial ecosystems will
90 respond to perturbations in soil nutrient dynamics (*e.g.*, from elevated nitrogen deposition
91 or CO_2 fertilization-induced nutrient requirements).
92 Intense competition between plants and microorganisms is a well-observed
93 phenomenon in nutrient-limited systems [*Hodge et al.*, 2000a; *Johnson*, 1992; *Kaye and*
94 *Hart*, 1997]. Previously, plants were thought to be initial losers in nutrient competition,
95 due to the fact that microbes are more intimately associated with substrates [*Woodmansee*
96 *et al.*, 1981]. However, increasing observational evidence indicates that plants compete
97 effectively with soil microorganisms [*Schimel and Bennett*, 2004] under certain
98 circumstances; sometime even outcompeting them and suppressing microbial growth [*Hu*
99 *et al.*, 2001; *J Wang and Lars*, 1997]. ^{15}N isotope studies have also demonstrated that
100 plants can capture a large fraction of added nitrogen [*Hodge et al.*, 2000b; *Marion et al.*,
101 1982]. In the short term (days to months), plants maintain their competitiveness mainly
102 through (1) establishing mycorrhizal fungi associations [*Drake et al.*, 2011; *Rillig et al.*,
103 1998], which help plants acquire organic and inorganic forms of nitrogen [*Hobbie and*
104 *Hobbie*, 2006; *Hodge and Fitter*, 2010] and (2) root exudation of extracellular enzymes

105 that decompose rhizosphere soil organic matter [*Phillips et al.*, 2011]. In the relatively
106 longer term (months to years), morphological adjustment occurs; for example, plants
107 allocate more carbon to fine roots to explore laterally and deeper [*Iversen et al.*, 2011;
108 *Jackson et al.*, 2009]. Finally, over the course of years to decades, plant succession can
109 occur [*Medvigy et al.*, 2009; *Moorcroft et al.*, 2001] and the new plant demography will
110 need to be considered to represent nutrient controls on this time scale.

111 Given these patterns from the observational literature, nutrient competition is
112 either absent or over-simplified in existing Earth System Models (ESMs). One common
113 representation of plant-microbe competition is that plants compete poorly against
114 microbes in resource acquisition. For example, the O-CN land model [*Zaehle and Friend*,
115 2010] assumes that soil decomposing microbes have the priority to immobilize soil
116 mineral nitrogen. After microbes meet their demands, the remaining nitrogen is then
117 available for plant uptake.

118 Another treatment in ESM land models is that microbial and plant nutrient
119 acquisition competitiveness is based on their relative demands. For example, CLM4CN
120 [*Thornton et al.*, 2007] assumes that the plant and microbial nitrogen demands are
121 satisfied simultaneously. Under nitrogen infertile conditions, all nitrogen demands in the
122 system are down-regulated proportional to the individual demands and subject to
123 available soil mineral nitrogen. This approach led to unrealistic diurnal cycles of gross
124 primary production (GPP), with midday depressions in GPP occurring because of
125 predicted diurnal depletion of the soil mineral nitrogen pool. Emergent impacts of this
126 conceptualization of nutrient constraints on GPP resulted in poor predictions compared to
127 observations, with smaller than observed plant C growth responses to N deposition

[*Thomas et al.*, 2013a] and larger than observed responses to N fertilization [*Thomas et al.*, 2013b]. Further, most biogeochemistry models not integrated in ESMs also adopt one of these approaches. For instance, Biome-BGC [*Running and Coughlan*, 1988], CENTURY [*Parton et al.*, 1988], CASA (Carnegie-Ames-Stanford Approach; [*Potter et al.*, 1993]) and the Terrestrial Ecosystem Model - TEM [*McGuire et al.*, 1992] assume that available nutrients preferentially satisfy the soil microbial immobilization demand.

We believe the two conceptualizations of competition used in ESMs substantially over-simplify competitive interactions between plants and microbes and lead to biases in carbon cycle predictions. To begin to address the problems with these simplified approaches, Tang and Riley (2013) showed that complex consumer-substrate networks can be represented with an approach (called Equilibrium Chemical Approximation (ECA) kinetics) that simultaneously resolves multiple demands for multiple substrates, and demonstrated that the approach was consistent with observed litter decomposition observations. ECA kinetics has also recently been applied to analyze the emergent temperature response of SOM decomposition, considering equilibrium, non-equilibrium, and enzyme temperature sensitivities and abiotic interactions with mineral surfaces [*Tang and Riley*, 2014]. We extend on that work here by presenting an implementation of ECA kinetics to represent competition for multiple soil nutrients in a multiple consumer environment. We note that this paper demonstrates a method to handle instantaneous competition in the complex soil-plant network, but a robust competition representation for climate-scale models will require representation of dynamic changes in plant allocation and plant composition.

The aim of this study is to provide a reliable nutrient competition approach applicable for land models integrated in ESMs. However, before integration into an ESM, the competition model needs to be carefully calibrated and independently tested against observational data. This paper will therefore focus on model development and evaluation at several tropical forest sites where observations are available. Our objectives are to: (1) develop a soil biogeochemistry model with multiple nutrients (*i.e.*, NH_4^+, NO_3^-, and PO_x (represented as the sum of PO_4^{3-}, HPO_4^{2-}, and $H_2PO_4^-$)) and multiple nutrient consumers (*i.e.*, decomposing microbes, plants, nitrifiers, denitrifiers, and mineral surfaces) competition using ECA kinetics [*Tang and Riley*, 2013; *Zhu and Riley*, 2015]; (2) constrain the model with *in situ* observational datasets of soil carbon, nitrogen, and phosphorus dynamics using a Markov Chain Monte Carlo (MCMC) approach; and (3) test model performance against nitrogen and phosphorus fertilization studies.

2 Method

2.1 Model development

The Nutrient COMpetition model (N-COM) is designed as a soil biogeochemistry model (Figure 1) to simulate soil carbon decomposition, nitrogen and phosphorus transformations, abiotic interactions, and plant demands. Although our ultimate goal is to incorporate N-COM into a decomposition model that represents active microbial activity as the primary driver of decomposition, we start here by presenting the N-COM approach using a Century-like [*Koven et al.*, 2013; *Parton et al.*, 1988] structure, with additions to account for phosphorus dynamics. In our approach, we calculate potential immobilization using literature-derived parameters (*e.g.*, *VMAX*, K_M) in a Michaelis-Menten (MM) kinetics framework. The potential immobilization is subsequently modified using the ECA competition method.

Five pools of soil organic Carbon (C), Nitrogen (N), and Phosphorus (P) are considered: Coarse Wood Debris (CWD), litter, fast Soil Organic Matter (SOM) pool, medium SOM pool, and slow SOM pool. Litter is further divided into three sub-groups: metabolic, cellulose, and lignin. The soil organic C, N, and P decomposition ($F_{C,j}^{dec}$, $F_{N,j}^{dec}$, $F_{P,j}^{dec}$) follow first-order decay:

$$F_{C,j}^{dec} = k_j C_j r_\theta r_T \quad (1)$$

$$F_{N,j}^{dec} = k_j N_j r_\theta r_T \quad (2)$$

$$F_{P,j}^{dec} = k_j P_j r_\theta r_T \quad (3)$$

where k_j is the rate constant of soil organic matter decay (s^{-1}); C_j, N_j, and P_j are pool sizes (g m^{-2}) of carbon, nitrogen, and phosphorus, respectively (*j* from 1 to 7 represents the soil organic matter pools: CWD, metabolic litter, cellulose litter, lignin litter, fast

SOC, median SOC, slow SOC); r_T and r_θ (dimensionless) are soil temperature and moisture environmental regulators.

Decomposed carbon ($F_{C,i}^{dec}$) (upstream i^{th} pool) either (1) enters a downstream pool (j^{th}) or (2) is lost as CO_2. Soil organic carbon (downstream j^{th} pool) temporal change is calculated as:

$$\frac{dC_j}{dt} = -F_{C,j}^{dec} + \sum_{i=1}^{N} F_{C,ij}^{move} \quad (4)$$

where $\sum_{i=1}^{N} F_{C,ij}^{move}$ is the summation of carbon fluxes that move from the upstream pool (i) to the downstream pool (j) due to the decomposition of upstream SOC. For each upstream carbon pool (i = *1, 2, ..., 7*), the fractions integrated into downstream pools (j = *1, 2, ..., 7*) is summarized in a 7×7 matrix f_{ij} (Table 2). The percentage of decomposed carbon that is respired as CO_2 is represented by g_i (Table 2). Simultaneously, soil organic N and P changes follow C decomposition:

$$\frac{dN_j}{dt} = -F_{N,j}^{dec} + \sum_{i=1}^{N} F_{N,ij}^{move} + \sum_{i=1}^{N} F_{NH4,ij}^{immob} + \sum_{i=1}^{N} F_{NO3,ij}^{immob} \quad (5)$$

$$\frac{dP_j}{dt} = -F_{P,j}^{dec} + \sum_{i=1}^{N} F_{P,ij}^{move} + \sum_{i=1}^{N} F_{P,ij}^{immob} \quad (6)$$

where $F_{N,ij}^{move}$ and $F_{P,ij}^{move}$ are fluxes of nitrogen and phosphorus moving from the upstream (i) to downstream (j) pools. $F_{NH4,ij}^{immob}$, $F_{NO3,ij}^{immob}$, and $F_{P.ij}^{immob}$ are immobilization fluxes of soil mineral nitrogen and phosphorus. $F_{N,j}^{dec}$ and $F_{P,j}^{dec}$ represent soil organic matter decomposition losses.

Equations (5) and (6) state that changes in the j^{th} organic N or P pool are the summation of three terms: (1) organic N and P lost during soil organic matter mineralization ($-F_{N,j}^{dec}$ and $-F_{P,j}^{dec}$); (2) a fraction of the i^{th} organic N or P pool (upstream) enters into the j^{th} pool (downstream) ($F_{N,ij}^{move}$ and $F_{P,ij}^{move}$); and (3) soil microbial immobilization ($F_{NH4,ij}^{immob}$, $F_{NO3,ij}^{immob}$, and $F_{P,ij}^{immob}$). Immobilization occurs only when the newly entering organic N is insufficient to sustain the soil C:N (or C:P) ratio (more details described in Appendix A).

The inorganic nitrogen pools (NH_4^+ and NO_3^- (Eqn. 7 -8)) are altered by production (organic N mobilized by microbes), consumption (uptake by plants and microbes, gaseous or aqueous losses), and transformation (nitrification and denitrification). Inorganic P (PO_x) is assumed to be either taken up by plants and decomposing microbes or adsorbed to mineral surfaces (Eqn. 9). Plants utilize all forms of phosphate (*e.g.*, PO_4^{3-}, HPO_4^{2-}, and $H_2PO_4^-$), but for simplicity we use the symbol PO_x to represent the sum of all possible phosphate forms throughout the paper.

$$\frac{d[NH4]}{dt} = \sum_{j=1}^{N}\sum_{i=1}^{N} F_{NH4,ij}^{mob} - F_{NH4}^{nit} - F_{NH4}^{plant} - F_{NH4}^{immob} + F^{BNF} + F_{NH4}^{dep} \quad (7)$$

$$\frac{d[NO3]}{dt} = -F_{NO3}^{den} + (1 - f^{N2O})F_{NH4}^{nit} - F_{NO3}^{plant} - F_{NO3}^{immob} - F_{NO3}^{leach} + F_{NO3}^{dep} \quad (8)$$

$$\frac{d[PO_x]}{dt} = \sum_{j=1}^{N}\sum_{i=1}^{N} F_{P,ij}^{mob} - F_P^{plant} - F_P^{immob} - F_P^{surf} - F_P^{leach} + F^{weather} \quad (9)$$

where $F_{NH4,ij}^{mob}$ and $F_{P,ij}^{mob}$ are gross mineralization rates for nitrogen and phosphorus. F_{NH4}^{nit} is the nitrification flux, part of which is lost through a gaseous pathway (f^{N2O}) and the rest is incorporated into the NO_3^- pool. F_{NO3}^{den} is the denitrification flux, which transforms nitrate to N_2O and N_2 which then leave the soil system. Plant uptake of soil NH_4^+, NO_3^-,

and PO_x are represented as F_{NH4}^{plant}, F_{NO3}^{plant}, and F_P^{plant}, respectively. Soil decomposing microbial immobilization of soil NH_4^+, NO_3^-, and PO_x are represented as F_{NH4}^{immob}, F_{NO3}^{immob}, and F_P^{immob}. F_{NO3}^{leach}, and F_P^{leach} are leaching losses of soil NO_3^- and PO_x. External inputs into soil inorganic N pools include atmospheric ammonia deposition (F_{NH4}^{dep}), atmospheric nitrate deposition (F_{NO3}^{dep}), and biological nitrogen fixation (F^{BNF}). External sources of phosphate come from parent material weathering ($F^{weather}$).

Finally, the dynamics of sorbed P (P_S), occluded P (P_O), and parent material P (P_P) are modeled as:

$$\frac{d[P_S]}{dt} = F_P^{surf} - F_P^{occl} \quad (10)$$

$$\frac{d[P_O]}{dt} = F_P^{occl} \quad (11)$$

$$\frac{d[P_P]}{dt} = -F^{weather} + F_P^{dep} \quad (12)$$

where the pool of sorbed P is balanced by the adsorption flux (F_P^{surf}) and occlusion flux (F_P^{occl}). Parent material is lost by weathering ($F^{weather}$) and is slowly replenished by external atmospheric phosphorus inputs (F_P^{dep}, such as dust). More detailed information on the modeled C, N, and P fluxes is documented in Appendix A.

2.2 Multiple-consumer-multiple-resource competition network

The soil biogeochemistry model presented in **section 2.1** has multiple potential nutrient consumers (plants, SOM decomposing microbes, nitrifiers, denitrifiers, mineral surfaces) and multiple soil nutrients (NH_4^+, NO_3^-, PO_x). The consumer-resource network is summarized in Table 1. As in many land BGC models (CLM, Century, *etc.*), we have

not explicitly included the mineral surface adsorptions of NH_4^+ and NO_3^-, since we assume ammonia is quickly protected by mineral surfaces from leaching (no leaching term in Eqn. 7) but then released for plant and microbial uptake when the biotic demand arises. An improved treatment of these dynamics would necessitate a prognostic model for pH, which is beyond the scope of this analysis. Unlike sorbed P (which can be occluded), there is no further abiotic loss of sorbed ammonia. Therefore, the free ammonia pool is interpreted in the current model structure as a potential free ammonia pool (free + sorbed).

Competition between different consumers in acquiring different resources is summarized in Table 1. Each consumer-substrate competition reaction is represented by:

$$S + E \underset{k_1^-}{\overset{k_1^+}{\rightleftharpoons}} C \xrightarrow{k_2^+} P + E \tag{13}$$

The enzyme (*E: e.g., nutrient carrier enzyme produced by plants and microbes*) and substrate (*S: e.g., NH_4^+, NO_3^-*) reaction (reversible reaction) forms a substrate-enzyme complex (*C*). The following irreversible reaction leads to product (*P: meaning the nutrients has been taken up*) and releases enzyme (*E*) back into soil media. For the whole complex reaction network, nutrient uptakes are formulated as:

$$F_{NH4}^{plant} = k_{NH4}^{plant} \cdot \frac{[NH4] \cdot [E_N^{plant}]}{K_M^{plant,NH4}\left(1 + \underbrace{\frac{[NH4]}{K_M^{plant,NH4}}}_{(1)} + \underbrace{\frac{[NO3]}{K_M^{plant,NO3}}}_{(2)} + \underbrace{\frac{[E_N^{plant}]}{K_M^{plant,NH4}}}_{(3)} + \underbrace{\frac{[E_N^{mic}]}{K_M^{mic,NH4}}}_{(4)} + \underbrace{\frac{[E_N^{nit}]}{K_M^{nit,NH4}}}_{(5)}\right)} \tag{14}$$

$$F_{NH4}^{immob} = k_{NH4}^{immob} \cdot \frac{[NH4] \cdot [E_N^{mic}]}{K_M^{mic,NH4}\left(1 + \frac{[NH4]}{K_M^{mic,NH4}} + \frac{[NO3]}{K_M^{mic,NO3}} + \frac{[E_N^{plant}]}{K_M^{plant,NH4}} + \frac{[E_N^{mic}]}{K_M^{mic,NH4}} + \frac{[E_N^{nit}]}{K_M^{nit,NH4}}\right)} \tag{15}$$

$$F_{NH4}^{nit} = k_{NH4}^{nit} \cdot \frac{[NH4] \cdot [E_{NH4}^{nit}]}{K_M^{nit,NH4}\left(1 + \frac{[NH4]}{K_M^{nit,NH4}} + \frac{[E_N^{plant}]}{K_M^{plant,NH4}} + \frac{[E_N^{mic}]}{K_M^{mic,NH4}} + \frac{[E_N^{nit}]}{K_M^{nit,NH4}}\right)} \tag{16}$$

$$F_{NO3}^{plant} = k_{NO3}^{plant} \cdot \frac{[NO3] \cdot [E_N^{plant}]}{K_M^{plant,NO3}(1 + \frac{[NH4]}{K_M^{plant,NH4}} + \frac{[NO3]}{K_M^{plant,NO3}} + \frac{[E_N^{plant}]}{K_M^{plant,NO3}} + \frac{[E_N^{mic}]}{K_M^{mic,NO3}} + \frac{[E_N^{den}]}{K_M^{den,NO3}})} \quad (17)$$

$$F_{NO3}^{immob} = k_{NO3}^{immob} \cdot \frac{[NO3] \cdot [E_N^{mic}]}{K_M^{mic,NO3}(1 + \frac{[NH4]}{K_M^{mic,NH4}} + \frac{[NO3]}{K_M^{mic,NO3}} + \frac{[E_N^{plant}]}{K_M^{plant,NO3}} + \frac{[E_N^{mic}]}{K_M^{mic,NO3}} + \frac{[E_N^{den}]}{K_M^{den,NO3}})} \quad (18)$$

$$F_{NO3}^{den} = k_{NO3}^{den} \cdot \frac{[NO3] \cdot [E_{NO3}^{den}]}{K_M^{den,NO3}(1 + \frac{[NO3]}{K_M^{den,NO3}} + \frac{[E_N^{plant}]}{K_M^{plant,NO3}} + \frac{[E_N^{mic}]}{K_M^{mic,NO3}} + \frac{[E_N^{den}]}{K_M^{den,NO3}})} \quad (19)$$

$$F_P^{plant} = k_P^{plant} \cdot \frac{[PO_x] \cdot [E_P^{plant}]}{K_M^{plant,P}(1 + \frac{[PO_x]}{K_M^{plant,P}} + \frac{[E_P^{plant}]}{K_M^{plant,P}} + \frac{[E_P^{mic}]}{K_M^{mic,P}} + \frac{[E_P^{surf}]}{K_M^{surf,P}})} \quad (20)$$

$$F_P^{mic} = k_P^{mic} \cdot \frac{[PO_x] \cdot [E_P^{mic}]}{K_M^{mic,P}(1 + \frac{[PO_x]}{K_M^{mic,P}} + \frac{[E_P^{plant}]}{K_M^{plant,P}} + \frac{[E_P^{mic}]}{K_M^{mic,P}} + \frac{[E_P^{surf}]}{K_M^{surf,P}})} \quad (21)$$

$$F_P^{surf} = k_P^{surf} \cdot \frac{[PO_x] \cdot [E_P^{mic}]}{K_M^{surf,P}(1 + \frac{[PO_x]}{K_M^{surf,P}} + \frac{[E_P^{plant}]}{K_M^{plant,P}} + \frac{[E_P^{mic}]}{K_M^{mic,P}} + \frac{[E_P^{surf}]}{K_M^{surf,P}})} \quad (22)$$

where F represent the nutrient uptake fluxes and k is the base reaction rate that enzyme-substrate complex forms product (k_2^+ in Eqn. 13). $[E]$ and K_M denote enzyme abundance and half saturation constants (substrate-enzyme affinity). Superscripts and subscripts refer to consumers and substrates, respectively. These equations account for the effect of (1) multiple substrates (*e.g.*, NH_4^+ and NO_3^-) sharing one consumer, which inhibits the effective binding between any specific substrate and the consumer (terms $^{(1)}$ and $^{(2)}$ in Eqn. 14) and (2) multiple consumers (*e.g.*, plants, decomposing microbes, and nitrifiers)

sharing one substrate (*e.g.*, NH_4^+), which lowers the probability of effective binding between any consumer and NH_4^+ (terms $^{(3)}$, $^{(4)}$, and $^{(5)}$ in Eqn. 14).

For our reaction network (Eqn. 13 – 22), we assume that: (1) plant roots and decomposing microbes possess two types of nutrient carrier enzymes (nutrient transporters). One is for nitrogen (NH_4^+ and NO_3^-; E_N^{plant}, E_N^{mic}), and the other is for phosphorus, including different forms of phosphate (E_P^{plant}, E_P^{mic}). (2) Nutrient carrier enzyme abundance is scaled with biomass (fine root or microbial biomass). Scaling factors are 0.0000125 (for plants) and 0.05 (for decomposing microbes) (Table 2). (3) Mineral surface "effective enzyme" abundance (E_P^{surf}) is approximated by the available sorption surface area ($VMAX_P^{surf} - [SP]$). (4) Nitrifiers and denitrifiers are not explicitly simulated, therefore we assume that their biomass and associated nutrient transporter abundance are fixed (E_N^{nit}, E_N^{denit}).

For simplicity, we group the "decomposing microbes/nitrifier/denitrifier/mineral surface nutrient carrier enzyme [*E*]" and their "base reaction rate *k*" into one single variable "*VMAX*" (see Appendix B for full derivation). Furthermore, we defined "potential rates (potential immoblizaiton, nitrification, denitrification, adsorption rates)" and used them as proxies of "*VMAX*". Therefore, Eqn. 15, 16, 18, 19, 21, 22 become:

$$F_{NH4}^{immob} = F_{NH4}^{immob,pot} \cdot \frac{[NH4]}{K_M^{mic,NH4}(1+\frac{[NH4]}{K_M^{mic,NH4}}+\frac{[NO3]}{K_M^{mic,NO3}}+\frac{[E_N^{plant}]}{K_M^{plant,NH4}}+\frac{[E_N^{mic}]}{K_M^{mic,NH4}}+\frac{[E_N^{nit}]}{K_M^{nit,NH4}})} \quad (23)$$

$$F_{NH4}^{nit} = F_{NH4}^{nit,pot} \cdot \frac{[NH4]}{K_M^{nit,NH4}(1+\frac{[NH4]}{K_M^{nit,NH4}}+\frac{[E_N^{plant}]}{K_M^{plant,NH4}}+\frac{[E_N^{mic}]}{K_M^{mic,NH4}}+\frac{[E_N^{nit}]}{K_M^{nit,NH4}})} \quad (24)$$

$$F_{NO3}^{immob} = F_{NO3}^{immob,pot} \cdot \frac{[NO3]}{K_M^{mic,NO3}(1+\frac{[NH4]}{K_M^{mic,NH4}}+\frac{[NO3]}{K_M^{mic,NO3}}+\frac{[E_N^{plant}]}{K_M^{plant,NO3}}+\frac{[E_N^{mic}]}{K_M^{mic,NO3}}+\frac{[E_N^{den}]}{K_M^{den,NO3}})} \quad (25)$$

$$F_{NO3}^{den} = F_{NO3}^{den,pot} \cdot \frac{[NO3]}{K_M^{den,NO3}(1+\frac{[NO3]}{K_M^{den,NO3}}+\frac{[E_N^{plant}]}{K_M^{plant,NO3}}+\frac{[E_N^{mic}]}{K_M^{mic,NO3}}+\frac{[E_N^{den}]}{K_M^{den,NO3}})} \quad (26)$$

$$F_P^{mic} = F_P^{immob,pot} \cdot \frac{[PO_x]}{K_M^{mic,P}(1+\frac{[PO_x]}{K_M^{mic,P}}+\frac{[E_P^{plant}]}{K_M^{plant,P}}+\frac{[E_P^{mic}]}{K_M^{mic,P}}+\frac{[E_P^{surf}]}{K_M^{surf,P}})} \quad (27)$$

$$F_P^{surf} = F_P^{surf,pot} \cdot \frac{[PO_x]}{K_M^{surf,P}(1+\frac{[PO_x]}{K_M^{surf,P}}+\frac{[E_P^{plant}]}{K_M^{plant,P}}+\frac{[E_P^{mic}]}{K_M^{mic,P}}+\frac{[E_P^{surf}]}{K_M^{surf,P}})} \quad (28)$$

In this case, the potential rates are treated as maximum reaction rates (*VMAX*), because they are calculated without nutrient constraints or biotic and abiotic interactions. For example, potential P immobilization rate ($F_P^{immob,pot}$) is based on the total phosphorus demand that can perfectly maintain the soil CP stoichiometry during soil organic matter decomposition (Eqn. A9). This potential immobilization rate represents the maximum phosphorus influx that the soil could take up at that moment. The maximum adsorption rate ($F_P^{surf,pot}$) is the time derivative of the Langmuir equation (Eqn. A12), which is a theoretically maximal adsorption rate excluding all other biotic and abiotic interactions. The potential rates (*VMAX*) are updated by the model rather than calibrated, except for $VMAX_P^{surf}$. $VMAX_P^{surf}$ denotes the maximum adsorption capacity (not maximum adsorption rate), which affects the potential adsorption rate ($F_P^{surf,pot}$).

The model is run on an hourly time step, initialized with state variables and critical parameters (Table 2). Since the model is designed to be a component of the

312 Community and ACME Land Models (CLM, ALM; which are essentially currently
313 equivalent), we used CLM4.5 site-level simulations to acquire temporally-resolved: (1)
314 soil temperature factors on decomposition (r_T); (2) soil moisture factors on
315 decomposition (r_θ); (3) the anoxic fraction of soil pores (f^{anox} in Appendix Eqn. A10-
316 11); (4) annual NPP (NPP_{annual} in Appendix Eqn. A13); (5) NH_4^+ deposition (F_{NH4}^{dep}); (6)
317 NO_3^- deposition (F_{NO3}^{dep}); and (7) hydrologic discharge (Q_{dis} in Appendix Eqn. A14).
318 External inputs of mineral phosphorus are derived from Mahowald *et al.*, [2005, 2008].

319 **2.3 Model parameterization and sensitivity analysis**

320 We constrained model parameters and performed sensitivity analyses using a suite
321 of observations distinct from the observations we used subsequently to test the model
322 against the N and P manipulation experiments. Because tropical systems can be either
323 nitrogen or phosphorous limited (or both) [*Elser et al.*, 2007; *Vitousek et al.*, 2010], we
324 chose observations from a tropical forest site to constrain the N and P competition in our
325 model (Tapajos National Forest, Para, Brazil (Table 3)).

326 In the parameter estimation procedure, several data streams are assimilated into
327 the N-COM model, including measurements of soil NH_4^+ concentrations, soil free
328 phosphate concentrations, sorbed phosphate concentrations, and N_2O and CO_2 flux
329 measurements. The datasets are summarized in Table 3 and cover a wide range of N and
330 P biogeochemistry dynamics. A set of model parameters is selected for calibration (Table
331 4), which comprise nutrient competition kinetics parameters (k and K_M) as well as the fast
332 soil carbon turnover time ($TURN_{SOM}$). Because we had only a short-term CO_2 respiration
333 flux record, we were unable to calibrate the longer turnover time parameters. However,
334 since we test the calibrated model against short-term fertilization responses, this omission

will not affect our evaluation. Longer records from eddy covariance flux towers and ^{14}C soil measurements are required to constrain the longer turnover time pool values.

We employed the Markov Chain Monte Carlo (MCMC) approach [*Ricciuto et al.*, 2008] to assimilate the observations into N-COM. MCMC directly draws samples from a pre-defined parameter space and tries to minimize a pre-defined cost function:

$$J = (M(\theta) - D)^T R^{-1} (M(\theta) - D) \quad (29)$$

where $\boldsymbol{M(\theta)}$ and $\boldsymbol{D}$ are vectors of model outputs and observations including time series of different simulated variables (*e.g.*, soil CO_2 and N_2O effluxes and soil concentrations of NH_4^+, free PO_x, and sorbed PO_x); $\boldsymbol{\theta}$ is a vector of model parameters ($\boldsymbol{\theta_i}$); and $\boldsymbol{i}$ from 1 to 20 represents the parameters that are calibrated (Table 4). R^{-1} is the inverse of data error covariance matrix. We assumed that diagonal elements are 40% of observed values and off-diagonal elements are zeros. We further assumed that the prior parameter follows a lognormal distribution. μ and σ were 0.91 and 0.95 of their initial values, respectively (Table 4). We then ran MCMC to sample 50,000 parameter pairs (Fig. A1). The second half of the samples was fit to a Gaussian distribution. We also employed the Gelman-Rubin criterion to quantitatively show whether or not the MCMC chain converged. The calibrated model parameters are reported in term of means and standard deviations. Uncertainty Reduction (*UR*) is calculated based on (1) variance (Eqn. 30a) and (2) 25% and 75% quantile (Eqn. 30b):

$$UR_\sigma = (1 - \frac{\sigma_{posterior}}{\sigma_{prior}}) \cdot 100\% \quad (30a)$$

$$UR_Q = (1 - \frac{Q^{75}_{posterior} - Q^{25}_{posterior}}{Q^{75}_{prior} - Q^{25}_{prior}}) \cdot 100\% \quad (30b)$$

where σ_{prior} is prior parameter uncertainty, which is 95% of the parameter initial value. $\sigma_{posterior}$ is calibrated parameter uncertainty, which is calculated by fitting the calibrated model parameters to a Gaussian distribution. Q^{75} and Q^{25} are 75% and 25% percentage quantile of each parameter. Uncertainty Reduction is a useful metric [*Zhu and Zhuang*, 2014], because it quantitatively reveals the reduction in the range of a particular parameter after calibration with MCMC. It does not, however, indicate that the parameter itself is more consistent with observed values of the parameter. A large value of *UR* implies a more robust model.

In addition, we conducted a sensitivity study to identify the dominant controlling factors regulating nutrient competition in N-COM. Three scenarios were considered: (1) baseline climate and soil conditions; (2) elevated soil temperature (by 5 °C); and (3) elevated soil moisture (by 50%). SOBOL sampling [*Pappas et al.*, 2013], a global sensitivity technique, is employed to calculate the sensitivities of output variables with respect to various inputs:

$$S_i = \frac{VAR_{p_i}(E_{p_{\sim i}}(Y \mid p_i))}{VAR(Y)} \tag{31}$$

where S_i is the first order sensitivity index of the i^{th} parameter and ranges from 0 to 1. By comparing the values of S_i, we were able to evaluate which processes affect the pattern of nutrient competition. Y represents the model outputs of plant NH_4^+, NO_3^-, or PO_x uptake; p_i is the target parameter; $p_{\sim i}$ denotes all parameters that are associated with nutrient competition except the target parameter; and *VAR(.)* and *E(.)* represent variance and mean, respectively.

2.4 Model application

After calibration, we applied the N-COM model to several tropical forest nutrient fertilization studies not included in the calibration dataset, where isotopically labeled nitrogen or phosphorous fertilizer was injected into the soil. The fertilization experiments measured the fate of added nutrients; for example, identifying the fraction of added N or P that goes into the plant, is immobilized by microbes, or is stabilized by mineral surfaces. These measurements offer an effective baseline to test whether the N-COM model captures short-term nutrient competition.

Because we have focused in this paper on applications in tropical forests, we choose three tropical forest fertilization experiments with (1) PO_4^{3-}; (2) NH_4^+; and (3) NO_3^- additions (Table 5). The PO_4^{3-} fertilization experiment [*Olander and Vitousek*, 2005] was conducted in three Hawaiian tropical forests along a soil chronosequence (300, 20000, and 4100000 year old soils) that were fertilized with 10 μg g^{-1} $^{32}PO_4^{3-}$, respectively, and microbial demand versus soil sorption was measured. We did not evaluate the role of plants in phosphorus competition for the Hawaii sites, since plant phosphorus uptake was not measured in those field studies. Our model discriminates the Hawaii sites along the chronosequence by setting distinct initial pool sizes (derived from [*Olander and Vitousek*, 2004; *Olander and Vitousek*, 2005]) of soil organic carbon, nitrogen and phosphorus, and soil parent material phosphorus.

We also used measurements from NH_4^+ and NO_3^- fertilization studies located at the Luquillo tropical forest in Puerto Rico [*Templer et al.*, 2008]. In that study, 4.6 μg g^{-1} $^{15}NH_4^+$ was added into the highly weathered tropical forest soil and the consumption of $^{15}NH_4^+$ by plant roots, decomposing microbes, and nitrifiers were measured. In the same study, 0.92 μg g^{-1} $^{15}NO_3^-$ was added to the soil and the plant uptake and microbial

401 immobilization was measured. The measurements were made 24 or 48 hours after the
402 fertilizers were added.
403 For the model scenarios, we (1) spun up the N-COM model for 100 years; (2)
404 perturbed the soil nutrient pool by the same amount as the fertilization; (3) ran the model
405 for 24 or 48 hours and calculated how much of the added nutrients were absorbed by
406 plants, microbes, or mineral surfaces; and (4) compared our model simulations with the
407 observed data to assess model predictability. The 100-year spin up simulation aimed at
408 eliminating the effects of imposed initial inorganic pool sizes on fertilization
409 experiments, rather than accumulating soil organic matter in the system, since we
410 initialized the soil organic carbon pools from CLM4.5 steady state predictions.
411
412 **3. Results and discussion**
413 **3.1 Calibrated model parameters**
414 Our best estimates (second half of the MCMC chain) of the selected model
415 parameters based on the observations at the Tapajos National Forest, Para, Brazil are
416 shown in Figure 2. We found that calibrated parameter samples were not heavily tailed
417 and they generally follow Gaussian distributions (Figure A3). In order to quantitatively
418 compare the calibrated parameter distributions with prior distributions, we fit parameter
419 samples to a Gaussian distribution and estimated its means and standard deviations
420 (Table 4).
421 Even though the parameter mean was improved, the uncertainty may still be
422 relatively large. In other words, a prognostic prediction based on these calibrated
423 parameters could be relatively uncertain [*Scholze et al.*, 2007], due to large uncertainty

associated with the calibrated parameters. Therefore, we calculated the variance-based Uncertainty Reduction (UR_{σ}) (Eqn. 30a) to evaluate model improvement in terms of parameter uncertainty. We found that parameters' uncertainties were reduced by 13%~98%. This calculation might either overestimate or underestimate the UR_{σ}, due to the fact that the calibrated parameters did not strictly follow Gaussian distributions. But the actual UR_{σ} should not be far from our estimates, because these samples were not widely spread across the potential parameter space (Figure 2). The least constrained parameter was k_{NO3}^{plant} (reaction rate of plant nitrogen carrier enzyme with NO_3^- substrate). Two other NO_3^- dynamics related parameters were also not well constrained: UR_{σ} of $K_M^{mic,NO3}$ (half-saturation constant for decomposing microbe NO_3^- immobilization) and $K_M^{den,NO3}$ (half-saturation constant for denitrifier NO_3^- consumption) were only 63% and 68%, respectively. Compared with NH_4^+ or PO_x competition related parameters, we concluded that parameters associated with NO_3^- competition were the least constrained in the model. This result was primarily due to the lack of NO_3^- pool size data, and secondarily due to the fact that NO_3^- was not the major nitrogen source for plant or decomposing microbes. We also provide quantile-based Uncertainty Reduction for reference (Table 4). The above-mentioned conclusions still hold with quantile-based UR_Q, although the quantile-based UR_Q is generally higher than variance-based UR_{σ}. One parameter was calibrated to be at the upper boundary of its prior ranges (k_P^{plant}), implying that this tropical plant is highly efficient in phosphorus uptake. Although we do not have direct kinetic parameter observations for the specific tropical species involved in our study, an inferred high phosphorus uptake efficiency is reasonable for tropical species

that have adapted to these phosphorus deficient environments [*Begum and Islam*, 2005; *FÖHse et al.*, 1988].

Convergence of model parameters is reported with the Gelman-Rubin criterion (Table 4 and Figure A2). Using this criterion, seven (out of twenty) parameters are found to converge (Gelman-Rubin <= 1.1). The lack of convergence of the remaining parameters is partly due to data paucity. In particular, starting from different prior values, MCMC calibrations may result in different models that give rise to similar model-data misfit (i.e., "equafinality" [*Tang and Zhuang*, 2008]). In this regard, high frequency measurements may improve model calibration (see more discussion in **section 3.3**). The non-convergence of model parameters implies an imperfect model. Therefore, for large-scale model application, more work on data collection, parameter tuning, and uncertainty analysis is needed. However, even with these caveats, the model predictability is reasonably good when applied to the tropical forest fertilization experiments described in Section 3.4.

Berkeley Lab 12/9/15 9:57 PM
Comment [1]: Added

We re-organize the right hand sides of Eqns. 14 – 22 to be the product of potential nutrient uptake rate and an ECA limitation term; for example for plant NH_4^+ uptake:

$$F_{NH4}^{plant} = k_{NH4}^{plant} \cdot ECA_{NH4}^{plant} \tag{32}$$

$$ECA_{NH4}^{plant} = \frac{[NH4]\cdot[E_N^{plant}]}{K_M^{plant,NH4}(1+\frac{[NH4]}{K_M^{plant,NH4}}+\frac{[NO3]}{K_M^{plant,NO3}}+\frac{[E_N^{plant}]}{K_M^{plant,NH4}}+\frac{[E_N^{mic}]}{K_M^{mic,NH4}}+\frac{[E_N^{nit}]}{K_M^{nit,NH4}})} \tag{33}$$

Other "consumer-substrate reactions" have similar forms. Under a nutrient abundant situation (*e.g.*, fertilized agriculture ecosystem), the relative competitiveness of each consumer (*ECA*) is dominated by its specific enzyme abundance ([*E*]). Under such conditions, substrate affinity is no longer a controlling factor. In contrast, under nutrient

468 limited conditions (*e.g.*, many natural ecosystems), ECA is dominated by the specific
469 enzyme abundance as well as the substrate affinity ($[E]/K_M$). Therefore, consumers could
470 either enable an alternative high affinity nutrient transporter system (low K_M) or exude
471 more enzyme to enhance competitiveness. For example, at the whole-soil scale it has
472 been shown that root spatial occupation (C_{froot}) determines a plant's competitiveness
473 when low soil nutrient diffusivity is limiting nutrient supply [*Raynaud and Leadley*,
474 2004]. Consistently, our results highlighted the dominant role of nutrient carrier enzyme
475 abundance (E proportional to C_{froot}) in controlling competition. If we further assumed
476 that plants, decomposing microbes, and nitrifiers enzyme abundances were
477 approximately equal, we will have that the relative their competitiveness in acquiring
478 NH_4^+ was about 4:10:9 ($1/K_M^{plant,NH4} : 1/K_M^{mic,NH4} : 1/K_M^{nit,NH4}$). However, such results
479 could not be easily generalized to other ecosystems, because they heavily relied on the
480 traits (affinity) of specific competitors. For a different ecosystem, those traits would be
481 drastically different due to the change of, *e.g.*, plant species composition and microbial
482 community structure. Even for the same ecosystem, those traits could be highly
483 heterogeneous. For example, the community structure of decomposing microbes could be
484 different in rhizosphere and bulk soil (with different K_M). However, in this work we
485 assumed a well-mixed environment (one soil column), in order to be consistent with
486 large-scale ecosystem models. Although beyond the scope of the current study, the
487 consequences of ignoring the rhizosphere versus bulk soil heterogeneity warrants further
488 investigation. Large-scale models aim to quantify ecosystem level dynamics, although
489 they are usually driven by parameters inferred from *in situ* field observations. In the
490 absence of a model that explicitly represents this spatial heterogeneity, it is difficult to

quantify the impacts of using inferred rhizosphere decomposer affinities on model predictions of the whole soil [*Schimel et al.*, 1989]. Furthermore, the assumption of well-mixed environment in large-scale model is an inevitable flaw, because of large computational demands and a lack of scale-aware parameters and model structures for large-scale models to run fine scale simulations.

Although in this study ECA was applied to a large-scale model, the competition framework is readily applicable to fine scale models that consider soil heterogeneity. In fine-scale models, bulk soil nutrient competition can occur only among different microbes because they are ubiquitous in the soil (*e.g.*, nitrifier versus microbial decomposer), while rhizosphere nutrient competition occurs among plants and microbes (*e.g.*, nitrifier versus microbial decomposer versus roots). This distinction implies that the competitiveness parameters we infer here for N-COM, which does not currently explicitly represent bulk versus rhizosphere processes, subsume the range of fine scale processes controlling nutrient uptake. More research is required to link these different model spatial scales, theory, and parameterizations.

Berkeley Lab 12/9/15 10:07 PM
Comment [2]: Added

Our modeling framework highlights the important concept that "competitiveness" is a dynamic property of the competition network, and more importantly that it is linked to competitor functional traits (affinity and nutrient carrier enzyme abundance). This concept is in contrast to the prevailing assumption underlying all major large-scale ecosystem models, which either assume "relative demand competitiveness for different nutrient consumers" [*Thornton et al.*, 2007] or "soil microbes outcompete plants" [*McGuire et al.*, 1992; *Parton et al.*, 1988]. Imposing such pre-defined orders of competitiveness neglects the diversity of nutrient competitors (plants and microbes) and

514 their differences in nutrient uptake capacity expressed by relevant functional traits. Our
515 model framework offers a theoretically consistent approach to account for the diversity of
516 nutrient competition in different competitor networks.

517 **3.2 Model sensitivity analysis**

518 Through sensitivity analysis, we separately investigated the factors controlling
519 plant NH_4^+, NO_3^-, and PO_x competition (Figure 3). Each sensitivity analysis consisted of
520 three scenarios: (1) normal conditions (control); (2) elevated soil temperature ($+T_s$); and
521 (3) elevated soil moisture ($+\theta$). The sensitivity analysis indicates that the model is highly
522 sensitive to kinetics parameters (*e.g.*, K_M). Furthermore, the model is consistently
523 sensitive to the same parameters across all temperature and moisture conditions. The
524 environment affects the nutrient competition primarily through altering the nutrient
525 abundance. Enhanced soil temperature and soil moisture accelerated soil organic carbon
526 turnover, thereby releasing more inorganic nutrient into the soil (gross mineralization).
527 However, the impacts on plant nutrient uptake are limited (Figure 3) because the
528 enhanced soil organic matter decay also requires higher immobilization fluxes to sustain
529 the soil organic matter CNP stoichiometry. The enhancement of net mineralization would
530 be limited, and therefore would not change soil nutrient status dramatically.

531 **3.3 Model performance**

532 The prior and calibrated models were compared against observational datasets of
533 pool sizes of soil free phosphate, sorbed phosphate, and NH_4^+, CO_2 efflux, and N_2O
534 efflux (Figure 4). We note that although we attempted to acquire as many datasets that
535 contained these five observations as possible, more observations in tropical ecosystems
536 would clearly improve the parameter estimates. For example, in the experiment we

analyzed, only three measurements of soil free phosphate were made during 1999. Many detailed dynamics are therefore missing and could impact our parameter estimates. The prior model predicted an increasing trend of soil free PO_x, which resulted from underestimates of plant P uptake (by underestimating of k_P^{plant}) and soil microbial P immobilization (by overestimating $K_M^{mic,P}$). The calibrated model captured the seasonal dynamics of soil free PO_x reasonably well: increases during the wet season and gradual decreasing during the dry season (August to November). The prior model also largely underestimated the seasonal variability of nitrogen dynamics and underestimated the NH_4^+ pool size due to overestimation of plant NH_4^+ uptake (k_{NH4}^{plant}). In addition, it also underestimated the denitrification N_2O emissions, because of an underestimation of NH_4^+ to NO_3^- transformation rate (k_{nit}). Consequently, there was not enough NO_3^- substrate to react with denitrifiers and release N_2O. The calibrated model, however, accurately reproduced the seasonal dynamics of both NH_4^+ pool sizes and soil N_2O emissions. There were small differences between the prior and calibrated model predictions of soil CO_2 emissions. The CO_2 and N_2O effluxes were more frequently observed at Tapajos National Forest during 1999 to 2001, compared with phosphorus data. Most of the measurements were collected during the wet season. Therefore the modeled CO_2 and N_2O emissions were largely improved by assimilating these datasets.

The model performance implies that after assimilating multiple datasets, our model predictions were improved over the prior model. However, it is clear that more observations of the metrics applied in our MCMC approach would benefit the model calibration. Unfortunately, because of our focus on tropical sites, we were unable to acquire more datasets that had the full suite of measurements required. Datasets of soil

nutrient pool sizes (*e.g.*, NO_3^-) and higher frequency sampling of those sparse measurements (*e.g.*, POx) would significantly benefit the model uncertainty reduction.

3.4 Model testing against nitrogen and phosphorus fertilization studies

To test the calibrated N-COM model, we conducted short-term numerical competition experiments (24-hour or 48-hour simulations) by manually imposing an input flux into nutrient pools equivalent to the N and P fertilization experiments described above and in Table 5. The simulated results were compared with observations from the field manipulations.

In the P addition experiments across the Hawaiian chronosequence, the partitioning of phosphate between microbes and mineral surfaces was well represented by the N-COM model in the intermediate (20K yr) and old (4.1M yr) sites (Figures 5b and 5c), with no significant differences between model predictions and observations. In the youngest Hawaiian site (300 yr; Figure 5a), the relative partitioning was correctly simulated, but the predicted PO_4^{3-} magnitudes were lower than observations. Our simulations indicated that at the young soil site the added P exceeded microbial demand, resulting in lower predicted microbial P uptake than observed. This discrepancy reflected a possible deficiency of first-order SOC decay models (as we used here), which implicitly treat microbes as a part of soil organic matter. Since microbial nutrient immobilization is strictly regulated by the SOC turnover rate in this type of model, external nutrient inputs will no longer affect microbial nutrient uptake if the inputs exceed potential microbial demand. We therefore believe that explicit Microbe-Enzyme models might be able to better explain the strong microbe PO_4^{3-} uptake signal observed at the young Hawaii fertilization experiment site. Microbial models explicitly simulate the dynamics of

583 microbial biomass, which might be able to capture the expected rapid growth of
584 microbial communities under conditions of improved substrate quality [*Kaspari et al.*,
585 2008; *Wieder et al.*, 2009].

586 In the Puerto Rican Luquillo forest nitrogen addition experiments, partitioning of
587 added ammonium between plants and heterotrophic bacteria was well captured by the N-
588 COM model, with no significant differences between model predictions and observations
589 (Figure 5d). However, the model underestimated nitrifier NH_4^+ uptake. NO_3^- competition
590 in this site was also relatively accurately predicted (Figure 5e), although the
591 measurements did not include denitrification. Model estimates of plant NO_3^- uptake and
592 microbial NO_3^- immobilization were consistent with the observed ranges, but we
593 highlight the large observational uncertainties, particularly for microbial NO_3^- uptake.

594 In the pseudo-first-order decomposition model we applied here to demonstrate the
595 ECA competition methodology, the soil organic matter C:N:P ratio also limited microbial
596 N and P uptake. For this type of decomposition model, stoichiometric differences
597 between soil organic matter and microbes are not dynamically simulated. Such a
598 simplification of soil and microbial stoichiometry favors large spatial scale model
599 structures over long temporal periods, but hampers prediction of microbial short-term
600 responses to N and P fertilization. For example, the observed difference between
601 microbial and soil C:P ratios can be as large as 6-fold [*Mooshammer et al.*, 2014; *Xu et*
602 *al.*, 2013]. Were that the case in the observations we applied, the potential soil P demand
603 calculated based on a fixed soil organic matter C:P ratio could be only 17% of that based
604 on microbial C:P ratio.

605 **3.5 Implications of ECA competition treatment**

606 Terrestrial ecosystem growth and function are continuously altered by climate
607 (*e.g.*, warming, drought; [*Chaves et al.*, 2003; *Springate and Kover*, 2014]), external
608 nutrient inputs (*e.g.*, N deposition; [*Matson et al.*, 2002; *Matson et al.*, 1999]), and
609 atmospheric composition (*e.g.*, CO_2 concentration; [*Norby et al.*, 2010; *Oren et al.*, 2001;
610 *Reich et al.*, 2006]). Improved understanding of the underlying mechanisms regulating
611 ecosystem responses to environmental changes has been obtained through *in situ* level to
612 large-scale and long-term manipulation experiments. For example, decade-long Free-Air
613 Carbon Dioxide Enrichment (FACE) experiments have revealed that nitrogen limitation
614 diminished the CO_2 fertilization effect of forests [*Norby et al.*, 2010] and grasslands
615 [*Reich and Hobbie*, 2013] ecosystems. However, fewer efforts have been made towards
616 incorporating the observed process-level knowledge into Earth System Models (ESMs).
617 Therefore, a major uncertainty that has limited the predictability of ESMs has been the
618 incomplete representation of soil nutrient dynamics [*Zaehle et al.*, 2014]. Even though
619 new soil nutrient cycle paradigms were proposed during recent decades [*Korsaeth et al.*,
620 2001; *Schimel and Bennett*, 2004], they were restricted to either conceptual models or
621 only applied to explain laboratory experiments.
622 Many large-scale terrestrial biogeochemistry models (*e.g.*, O-CN, CASA, TEM)
623 have adopted the classical paradigm that microbes decompose soil organic matter and
624 release NH_4^+ as a "waste" product [*Waksman*, 1931]. The rate of this process is defined
625 as "net N mineralization", and is adopted as a "measure" of plant available inorganic N
626 [*Schimel and Bennett*, 2004]. This classical paradigm overlooked the fact that "net N
627 mineralization" actually comprised two individual processes - gross N mineralization and
628 microbial N immobilization. Implicitly, the classical paradigm assumes that the microbes

have priority to assimilate as much of the available nutrient pool as possible. Soil nutrients were only available for plant uptake if there were not enough free energy materials (*e.g.*, dissolved soil organic carbon) to support microbial metabolism. As a result, soil microbes were considered "victors" in the short-term nutrient competition. Some other large-scale terrestrial biogeochemistry models (*e.g.*, CLM4CN), simplify the concept of nutrient competition differently. They calculate the plant N uptake and soil N immobilization separately; and then down-regulate the two fluxes according to the soil mineral N availability. As a result, plant and soil microbe competitiveness for nutrients is determined by their relative demand.

Climate-scale land models have over-simplified or ignored competition between plants, microbes, and abiotic mechanisms. In reality, under high nutrient stress conditions, plants can exude nutrient carrier enzymes or facilitate mycorrhizal fungi associations to enhance competitiveness for nutrient acquisition [*Drake et al.*, 2011; *Hobbie and Hobbie*, 2006; *Treseder and Vitousek*, 2001]. In addition, plants can adjust C allocation to construct more fine roots, which scavenge nutrients over larger soil volumes [*Iversen et al.*, 2011; *Jackson et al.*, 2009; *Norby et al.*, 2004]. Soil spatial heterogeneity might also contribute to the success of plant nutrient competition [*Korsaeth et al.*, 2001]. Therefore, most ecosystem biogeochemistry models with traditional treatments of nutrient competition likely underestimate plant nutrient uptake.

Nutrient competition should be treated as a complex consumer-substrate reaction network: multiple 'consumers', including plant roots, soil heterotrophic microbes, nitrifiers, denitrifiers, and mineral surfaces, each competing for substrates of organic and inorganic nitrogen and phosphorus as nutrient supply. In such a model structure, the

652 success of any consumer in substrate acquisition is affected by its consumer-substrate
653 affinity [*Nedwell*, 1999]. Such competitive interactions have been successfully applied to
654 microbe-microbe and plant-microbe substrate competition modeling [*Bonachela et al.*,
655 2011; *Lambers et al.*, 2009; *Maggi et al.*, 2008; *Maggi and Riley*, 2009; *Moorhead and*
656 *Sinsabaugh*, 2006; *Reynolds and Pacala*, 1993] for many years.

657 Here, we applied the consumer-substrate network in a broader context of plant,
658 microorganism, and abiotic mineral interactions. We analyzed the consumer-substrate
659 network using a first-order accurate equilibrium chemistry approximation (ECA) [*Tang*
660 *and Riley*, 2013; *Zhu and Riley*, 2015]. Our sensitivity analysis confirmed that the
661 consumer-substrate affinity and nutrient carrier enzyme abundance were the most
662 important factors regulating relatively short-term competitive interactions. The ECA
663 competition treatment represents ecosystem responses to environmental changes and has
664 the potential to be linked to a microbe-explicit land biogeochemistry model. The
665 approach allows competition between plants, microbes, and mineral surfaces to be
666 prognostically determined based on nutrient status and capabilities of each consumer.
667

668 **4. Conclusions**

669 In this study, we developed a soil biogeochemistry model (N-COM) that resolves
670 the dynamics of soil nitrogen and phosphorus, plant uptake of nutrients, microbial uptake,
671 and abiotic interactions. We focused on the implementation, parameterization, and testing
672 of the nutrient competition scheme that we plan to incorporate into the ESM land models
673 CLM and ALM. We described the multiple-consumer and multiple-nutrient competition
674 network with the Equilibrium Chemical Approximation (ECA) [*Tang and Riley*, 2013]

675 considering two inhibitive effects: (1) multiple substrates (*e.g.*, NH_4^+ and NO_3^-) sharing
676 one consumer inhibits the effective binding between any specific substrate and the
677 consumer and (2) multiple consumers (*e.g.*, plants, decomposing microbes, nitrifers)
678 sharing one substrate (*e.g.*, NH_4^+) lowers the probability of effective binding between any
679 consumer and that substrate. We calibrated the model at a tropical forest site with highly
680 weathered soil (Tapajos National Forest, Para, Brazil), using multiple observational
681 datasets with the Markov Chain Monte Carlo (MCMC) approach. The calibrated model
682 compared to multiple categories of observational data was substantially improved over
683 the prior model (Figure 4). The seasonal dynamics of soil carbon, nitrogen, and
684 phosphorus were moderately well captured. However, our results would likely be more
685 robust if more temporally resolved observations of carbon, nitrogen, and phosphorous
686 were available. Although the calibrated model is the best one we can derive based on
687 limited data, several model parameters were not well converged. We therefore conclude
688 that more work on data collection, parameter tuning, and uncertainty analysis is needed.
689 To test the resulting model using the calibrated parameters, we applied N-COM to
690 two other tropical forests (Hawaii tropical forest and Luquillo tropical forest) not used in
691 the calibration process and conducted nutrient perturbation studies consistent with
692 fertilization experiments at these sites. The results showed that N-COM simulated the
693 nitrogen and phosphorus competition well for the majority of the observational metrics.
694 However, the model underestimated NH_4^+ uptake by nitrifiers, probably due to the
695 loosely constrained nitrification parameters that were the result of NO_3^- pool size data
696 paucity during calibration at the Brazil site (Table 4). Datasets of soil nutrient pool sizes

Berkeley Lab 12/9/15 9:58 PM
Comment [3]: Added

and CO_2 and N_2O effluxes with high frequency sampling would significantly benefit the model uncertainty reduction.

To date, many terrestrial ecosystem biogeochemistry models assume microbes outcompete plants and immobilize nutrients first [*Y P Wang et al.*, 2007; *Zaehle and Friend*, 2010; *Zhu and Zhuang*, 2013], although CLM currently assumes constant and relative demand competitiveness of plants and microbes. Few models, to our knowledge, consider the role of abiotic interactions in the competitive interactions. In the case of microbes outcompeting plants, the plant is only able to utilize the nutrients that exceed microbial demands during that time step. The leftover nutrients are defined as net mineralization, which is a widely adopted concept in soil biogeochemistry modeling [*Schimel and Bennett*, 2004]. These models oversimplify plant-microbe interactions by imposing dubious assumptions (*e.g.*, microbes always win against plants). We showed that (in section 3.1) "competitiveness" is a dynamic rather than fixed property of the competition network, and more importantly, it should be linked to competitor functional traits (affinity and nutrient carrier enzyme abundance).

This study is an important step towards implementing more realistic nutrient competition schemes in complex climate-scale land models. Traditional ESMs generally lack realistic soil nutrient competition, which likely biases the estimates of terrestrial ecosystem carbon productivity and biosphere-climate feedbacks. This study showed the effectiveness of ECA kinetics in representing soil multiple-consumer and multiple-nutrient competition networks. Offline calibration and independent site-level testing is critically important to ensuring the newly incorporated model will perform reasonably when integrated in a complex ESM. To this end, we provide a universal calibration

720 approach using MCMC, which could in the future be used to further constrain N-COM
721 across plant functional types, climate, and soil types.
722
723 *Acknowledgements:* This research was supported by the Director, Office of Science,
724 Office of Biological and Environmental Research of the US Department of Energy under
725 Contract No. DE-AC02-05CH11231 as part of the Regional and Global Climate
726 Modeling (RGCM) and ACME programs.

Figure 1. Model structure. Boxes represent pools, solid arrows represent aqueous fluxes, and dashed arrows represent gaseous pathways out or into the system. Three essential chemical elements (Carbon (C), Nitrogen (N) and Phosphorus (P)) are simulated in N-COM (blue, red, and green represent C, N, and P pools and processes, respectively).

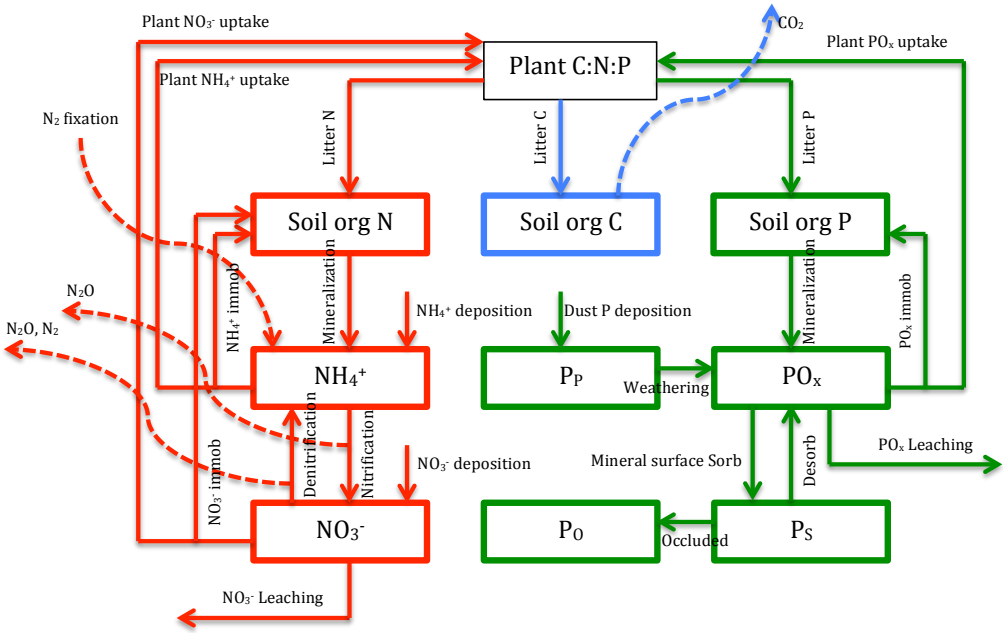

Figure 2. Distribution of prior and calibrated model parameters.

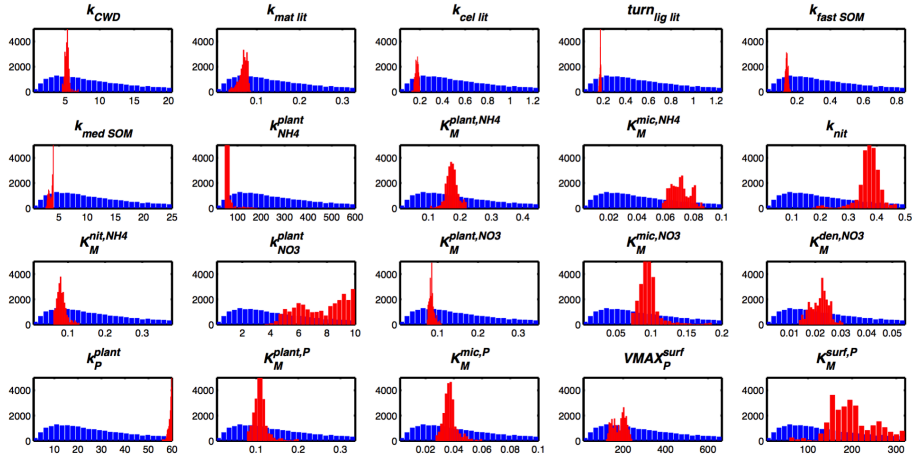

Figure 3. Model sensitivity analysis with SOBOL sampling. For each metric, three scenarios are shown: baseline (Control), elevated soil temperature by 5 °C ($+T_s$), and elevated soil moisture by 50% ($+\theta$), respectively. The length of bar (plot in polar coordinate) is the sensitivity (unit-less) of model output with respect to model input variables. Our results showed that the plant nutrient uptake was mostly regulated by internal consumer-substrate uptake kinetics rather than the external environmental conditions (*e.g.*, T_s, θ).

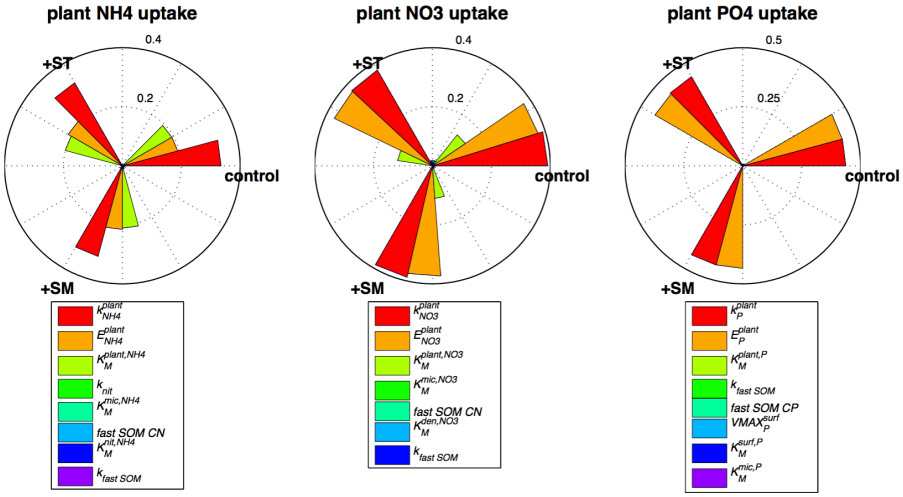

Figure 4. Model performance at Tapajos National Forest, Para, Brazil. Overall, the calibrated model (blue line) improved predictions over the prior model (grey line) when compared to observations. Green areas indicate the calibrated model uncertainties.

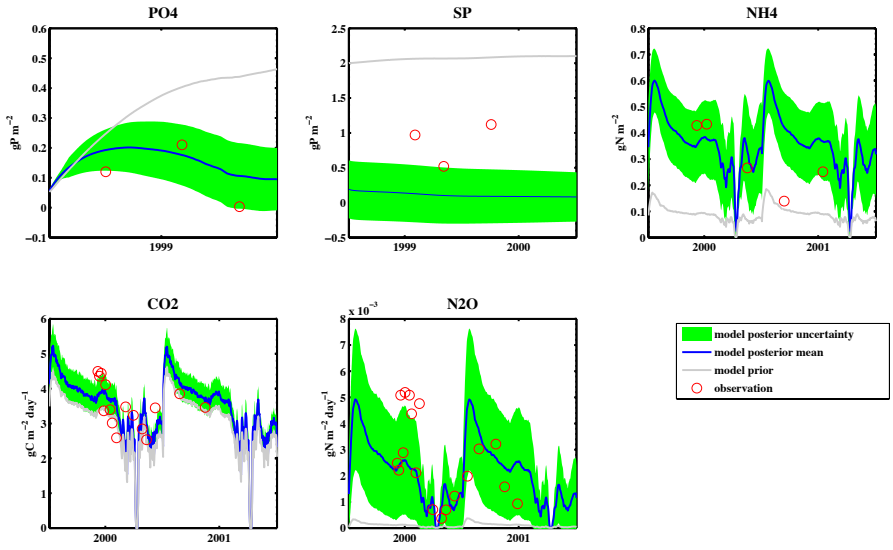

748 **Figure 5.** Model perturbation experiments compared with nitrogen and phosphorus
749 fertilization field experimental data. The blue dots show the difference between control
750 and perturbed simulations, which mean how much newly added nutrient each consumer
751 takes up. The red circles are recovered isotopically labeled nutrient within each
752 consumer. Since plants phosphorus uptake was not measured at Hawaii sites, we didn't
753 include the plants in the perturbation study.
754

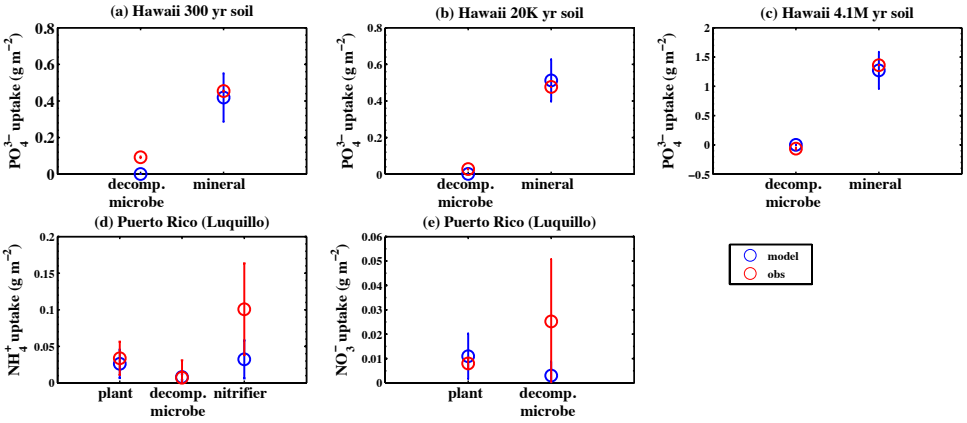

755 **Table 1.** A summary of the modeled consumer-resource competition network.

Resources	**Consumers**		
NH_4^+	Plant	Decomposing Microbe	Nitrifier
NO_3^-	Plant	Decomposing Microbe	Denitrifier
PO_x	Plant	Decomposing Microbe	Mineral surface

756

757 **Table 2.** Model parameters and baseline values.

C associated				
g_i	Percentage of carbon remains in the soil after decomposition of i^{th} SOM	-	[1.0; 0.45; 0.5; 0.5; 0.83; 0.45; 0.45]	[*Koven et al.*, 2013]
f_{ij}	fraction of SOM leave from i^{th} pool and enter into j^{th} pool	-	[0, 0, 0.76, 0.24, 0, 0, 0; 0, 0, 0, 0, 1, 0, 0; 0, 0, 0, 0, 1, 0, 0; 0, 0, 0, 0, 0, 1, 0; 0, 0, 0, 0, 0, 0.995, 0.005; 0, 0, 0, 0, 0.93, 0, 0.07; 0, 0, 0, 0, 1, 0, 0]	[*Koven et al.*, 2013]
CN	Soil organic matter CN ratio	-	[13,16,7.9]	[*Parton et al.*, 1988]
CP	Soil organic matter CP ratio	-	[110,320,114]	[*Parton et al.*, 1988]
$TURN_{SOM}$	Soil organic matter turn over [CWD, metabolic lit, cellulose lit, lignin lit, fast SOM, medium SOM, slow SOM]	year	[4.1, 0.066, 0.25, 0.25, 0.17, 5, 270]	[*Koven et al.*, 2013]
N associated				
k_{NH4}^{plant}	Reaction rate of plant NH_4^+ carrier enzyme	day^{-1}	120 [(a)]	[*Jackson et al.*, 1997; *Min et al.*, 2000]
$K_M^{plant,NH4}$	Half-saturation constant for plant NH_4^+ uptake	$g\ m^{-2}$	0.09	[*Kuzyakov and Xu*, 2013]
$K_M^{mic,NH4}$	Half-saturation constant for decomposing microbe NH_4^+ immobilization	$g\ m^{-2}$	0.02	[*Kuzyakov and Xu*, 2013]
k_{nit}	Maximum fraction of NH_4^+ pool that could be utilized by nitrifiers	day^{-1}	10%	[*Parton et al.*, 2001]
$K_M^{nit,NH4}$	Half-saturation constant for nitrifier NH_4^+ consumption	$g\ m^{-2}$	0.076	[*Drtil et al.*, 1993]
k_{NO3}^{plant}	Reaction rate of plant NO_3^- carrier enzyme	day^{-1}	2 [(a)]	[*Jackson et al.*, 1997; *Min et al.*, 2000]
$K_M^{plant,NO3}$	Half-saturation constant for plant NO_3^- uptake	$g\ m^{-2}$	0.07	[*Kuzyakov and Xu*, 2013]
$K_M^{mic,NO3}$	Half-saturation constant for decomposing microbe NO_3^- immobilization	$g\ m^{-2}$	0.04	[*Kuzyakov and Xu*, 2013]
$K_M^{den,NO3}$	Half-saturation constant for denitrifier NO_3^- consumption	$g\ m^{-2}$	0.011	[*Murray et al.*, 1989]
$[E_N^{plant}]$	Plant nitrogen carrier enzyme abundance for nitrogen uptake	$g\ m^{-2}$	$C_{froot} \cdot 0.0000125$ [(a)]	[*Tang and Riley*, 2013; *Trumbore et al.*, 2006]
$[E_N^{mic}]$	Decomposing microbes nitrogen carrier enzyme abundance for nitrogen immobilization	$g\ m^{-2}$	$\frac{F_N^{immob,pot}}{1000}$ [(b)]	[*Tang and Riley*, 2013]
$[E_N^{nit}]$	Nitrifier nitrogen carrier enzyme abundance for NH_4^+ assimilation	$g\ m^{-2}$	$1.2E^{-3}$	[*Raynaud et al.*, 2006]

$[E_N^{den}]$	Denitrifier nitrogen carrier enzyme abundance for NO_3^- assimilation	g m^{-2}	1.2E^{-3}	[*Raynaud et al.*, 2006]
f^{N2O}	Fraction of nitrification flux lost as N_2O	-	6E^{-4}	[*Li et al.*, 2000]
P associated				
$k_{weather}$	Parent material P weathering rate	g P m^{-2} year^{-1}	0.004	[*Y P Wang et al.*, 2010]
k_{occl}	P occlude rate	month^{-1}	1.0E^{-6}	[*Yang et al.*, 2014]
k_P^{plant}	Reaction rate of plant PO_x carrier enzyme	day^{-1}	12 (a)	[*Colpaert et al.*, 1999]
$K_M^{plant,P}$	Half-saturation constant for plant PO_x uptake	g m^{-2}	0.067	[*Cogliatti and Clarkson*, 1983]
$K_M^{mic,P}$	Half-saturation constant for decomposing microbe PO_x immobilization	g m^{-2}	0.02	[*Chen*, 1974]
$VMAX_P^{surf}$	Maximum mineral surface PO_x adsorption	g m^{-2}	133	[*Y P Wang et al.*, 2010]
$K_M^{surf,P}$	Half-saturation constant for mineral surface PO_x adsorption	g m^{-2}	64	[*Y P Wang et al.*, 2010]
$[E_P^{plant}]$	Plant phosphorus carrier enzyme abundance for PO_x uptake	g m^{-2}	$C_{froot} \cdot 0.0000125$ (a)	[*Tang and Riley*, 2013; *Trumbore et al.*, 2006]
$[E_P^{mic}]$	Decomposing microbes phosphorus carrier enzyme abundance for PO_x immobilization	g m^{-2}	$\frac{F_P^{immob,pot}}{800}$ (b)	[*Tang and Riley*, 2013]
$[E_P^{surf}]$	Mineral surface "effective enzyme" abundance for PO_x adsorption	g m^{-2}	$VMAX_P^{surf} - [SP]$	[*Tang and Riley*, 2013]

(a) The scaling factor for plant nutrient enzyme abundance is 0.0000125. This number is inferred by assuming that growing season plant nutrient carrier enzymes are roughly the same order of magnitude compared with decomposing microbes'. Typical values for soil decomposing microbe biomass and tropical forest fine root biomass are 0.1 [*Tang and Riley*, 2013] and 400 [*Trumbore et al.*, 2006] gC m^{-2}. A typical value of scaling factor that scales microbial biomass to enzyme abundance is 0.05 [*Tang and Riley*, 2013]. Therefore, $C_{froot} \cdot x = C_{mic} \cdot 0.05$ or $400 \cdot x = 0.1 \cdot 0.05$. We have $x = 0.0000125$. Further, we have $k_{NH4}^{plant} \cdot [E_N^{plant}] = VMAX_{NH4}^{plant}$. We know that typical values for $VMAX_{NH4}^{plant}$ and $[E_N^{plant}]$ are 0.6 g m^{-2} day^{-1} [*Min et al.*, 2000] and 0.005 g m^{-2}. Then we have $k_{NH4}^{plant} = 120$ day^{-1}. Similarly, we have $k_{NO3}^{plant} \cdot [E_N^{plant}] = VMAX_{NO3}^{plant}$, $k_P^{plant} \cdot [E_P^{plant}] = VMAX_P^{plant}$. Knowing that typical values for $VMAX_{NO3}^{plant}$ and $VMAX_P^{plant}$ are 0.01 [*Min et al.*, 2000] and 0.06 [*Colpaert et al.*, 1999] g m^{-2} day^{-1}, we have $k_{NO3}^{plant} = 2$ and $k_P^{plant} = 12$ day^{-1}.

(b) For decomposing microbes, we have $VMAX_N^{mic} = k_N^{mic} \cdot [E_N^{mic}]$. Typical values for $VMAX_N^{immob}$ and $[E_N^{mic}]$ are 5 g m^{-2} day^{-1} [*Kuzyakov and Xu*, 2013] and 0.005 g m^{-2} [*Tang and Riley*, 2013]. Therefore, we have $k_N^{mic} = 1000$. Since our model calculates potential N immobilization rates and approximates them as $VMAX_N^{mic}$. The changes of potential N immobilization rates at each time step imply the changes of enzyme abundance through $[E_N^{mic}] = \frac{F_N^{immob,pot}}{k_N^{mic}} = \frac{F_N^{immob,pot}}{1000}$. Similarly, we have that $VMAX_P^{immob}$ and $[E_N^{mic}]$ are 2 g m^{-2} day^{-1} [*Chen*, 1974] and 0.005 g m^{-2}. Therefore, $k_P^{mic} = 800$ and $E_P^{mic} = \frac{F_P^{immob,pot}}{800}$.

760 **Table 3.** Observational datasets used for calibration. Number of observations for each data stream is included in brackets.

Processes	Datasets		Location	References
C associated	Soil heterotrophic respiration (20)		Tapajos National Forest, Para, Brazil	[*Silver et al.*, 2012]
N associated	Soil NH_4^+ (5)	N_2O efflux (20)	Tapajos National Forest, Para, Brazil	[*Silver et al.*, 2012]
P associated	Soil free phosphate (3)	Sorb phosphate (3)	Tapajos National Forest, Para, Brazil	[*McGroddy et al.*, 2008]

761

762 **Table 4.** Calibrated parameters are reported in terms of (1) mean/standard deviation by fitting to a Gaussian distribution; (2) 25% and

763 75% quantile. Both variance-based and quantile-based parameters uncertainty reduction are provided; (3) Gelman-Rubin convergence

764 criterion.

Berkeley Lab 12/9/15 9:59 PM
Comment [4]: Modified

Parameters	μ_{prior}	σ_{prior}	$\mu_{posterior}$	$\sigma_{posterior}$	**UR**	Q^{25}_{prior}	Q^{75}_{prior}	$Q^{25}_{posterior}$	$Q^{75}_{posterior}$	**UR**	**Gelman-Rubin criterion**
$TURN_{SOM}$	[3.7,	[3.9,	[5.2,	[0.33,	[92, 83,	[5.33,	[19.32,	[5.05, 0.63,	[5.39, 0.076,	[97, 94, 97, 99,	[1.69, 1.03, 1.75,
[CWD,	0.06,	0.06,	0.07,	0.01,	96, 98,	0.086, 0.33,	0.31, 1.18,	0.16, 0.17, 0.13,	0.18, 0.18, 0.14,	98, 96	1.01, 1.06, 1.55]
metabolic,	0.23,	0.24,	0.17,	0.01,	96, 92]	0.33, 0.22,	1.18, 0.8,	3.2]	3.9]		
cellulose, lignin	0.23,0.16,	0.24,	0.17,	0.005,		6.5]	23.5]				
lit, fast, medium	4.6]	0.18, 4.8]	0.14, 3.6]	0.008,							
SOM]				0.37]							
k^{plant}_{NH4}	109	114	58	14	88	156.1	565.4	52.8	60.0	98	1.87
$K^{plant,NH4}_{M}$	0.082	0.086	0.173	0.018	79	0.12	0.42	0.16	0.18	93	2.86
$K^{mic,NH4}_{M}$	0.018	0.019	0.071	0.0067	65	0.026	0.094	0.065	0.076	85	1.94
k_{nit}	0.091	0.095	0.37	0.038	60	0.13	0.47	0.36	0.39	91	2.02
$K^{nit,NH4}_{M}$	0.069	0.072	0.082	0.012	83	0.10	0.36	0.07	0.09	94	1.95
k^{plant}_{NO3}	1.8	1.9	7.6	1.7	13	2.60	9.42	6.11	9.14	56	1.01

$K_M^{plant,NO3}$	0.064	0.067	0.085	0.0064	90	0.09	0.33	0.08	0.09	97	3.17
$K_M^{mic,NO3}$	0.036	0.038	0.096	0.014	63	0.05	0.19	0.09	0.10	92	2.64
$K_M^{den,NO3}$	0.0101	0.0105	0.022	0.0034	68	0.014	0.052	0.019	0.024	87	1.03
k_P^{plant}	11	11.5	59	0.75	93	15.61	56.54	58.86	59.81	98	1.06
$K_M^{plant,P}$	0.061	0.064	0.11	0.015	77	0.09	0.32	0.10	0.12	94	1.52
$K_M^{mic,P}$	0.018	0.019	0.037	0.0047	75	0.026	0.094	0.034	0.039	93	2.86
$VMAX_P^{surf}$	121	127	182	30	76	173.0	626.6	156.5	206.3	89	2.25
$K_M^{surf,P}$	64	58	200	50	18	83.2	301.5	162.6	233.0	68	1.05

765

766 **Table 5.** Short-term (24 or 48 hours) fertilization experiments of NH_4^+, NO_3^-, or PO_4^{3-} additions used to evaluate the performance of

767 the N-COM competition scheme.

Datasets	Added nutrient	Competitors			Duration (hour)	References
PO_4^{3-} fertilization	10 μg g^{-1}	I. Mineral surface	II. Decomposing microbe		48	[*Olander and Vitousek*, 2005]
NH_4^+ fertilization	4.6 μg g^{-1}	I. Plant	II. Decomposing microbe	III. Nitrifier	24	[*Templer et al.*, 2008]
NO_3^- fertilization	0.92 μg g^{-1}	I. Plant	II. Decomposing microbe		24	[*Templer et al.*, 2008]

768

References:

Anav, A., P. Friedlingstein, M. Kidston, L. Bopp, P. Ciais, P. Cox, C. Jones, M. Jung, R. Myneni, and Z. Zhu (2013), Evaluating the land and ocean components of the global carbon cycle in the CMIP5 Earth System Models, *Journal of Climate*, *26*(18), 6801-6843.

Begum, H. H., and M. T. Islam (2005), Role of synthesis and exudation of organic acids in phosphorus nutrition in plants in tropical soils, *Biotechnology*, *4*(4), 333-340.

Bonachela, J. A., M. Raghib, and S. A. Levin (2011), Dynamic model of flexible phytoplankton nutrient uptake, *Proceedings of the National Academy of Sciences*, *108*(51), 20633-20638.

Bonan, G. B., and K. V. Cleve (1992), Soil temperature, nitrogen mineralization, and carbon source-sink relationships in boreal forests, *Canadian Journal of Forest Research*, *22*(5), 629-639.

Chauhan, B. S., J. W. B. Stewart, and E. A. Paul (1981), Effect of labile inorganic phosphate status and organic carbon additions on the microbial uptake of phosphorus in soils, *Canadian Journal of Soil Science*, *61*(2), 373-385.

Chaves, M. M., J. P. Maroco, and J. S. Pereira (2003), Understanding plant responses to drought—from genes to the whole plant, *Functional plant biology*, *30*(3), 239-264.

Chen, M. (1974), Kinetics of phosphorus absorption byCorynebacterium bovis, *Microbial ecology*, *1*(1), 164-175.

791 Cogliatti, D. H., and D. T. Clarkson (1983), Physiological changes in, and phosphate
792 uptake by potato plants during development of, and recovery from
793 phosphate deficiency, *Physiologia plantarum*, *58*(3), 287-294.
794 Colpaert, J. V., K. K. Van Tichelen, J. A. Van Assche, and A. Van Laere (1999), Short-
795 term phosphorus uptake rates in mycorrhizal and non-mycorrhizal roots of
796 intact Pinus sylvestris seedlings, *New Phytologist*, *143*(3), 589-597.
797 DeLuca, T. H., O. Zackrisson, M. J. Gundale, and M.-C. Nilsson (2008), Ecosystem
798 feedbacks and nitrogen fixation in boreal forests, *Science*, *320*(5880), 1181-
799 1181.
800 DeLuca, T. H., O. Zackrisson, M.-C. Nilsson, and A. Sellstedt (2002), Quantifying
801 nitrogen-fixation in feather moss carpets of boreal forests, *Nature*,
802 *419*(6910), 917-920.
803 Dise, N. B., and R. F. Wright (1995), Nitrogen leaching from European forests in
804 relation to nitrogen deposition, *Forest Ecology and Management*, *71*(1), 153-
805 161.
806 Drake, J. E., A. Gallet‐Budynek, K. S. Hofmockel, E. S. Bernhardt, S. A. Billings, R. B.
807 Jackson, K. S. Johnsen, J. Lichter, H. R. McCarthy, and M. L. McCormack (2011),
808 Increases in the flux of carbon belowground stimulate nitrogen uptake and
809 sustain the long‐term enhancement of forest productivity under elevated
810 CO2, *Ecology letters*, *14*(4), 349-357.
811 Drtil, M., P. Nemeth, and I. Bodik (1993), Kinetic constants of nitrification, *Water*
812 *Research*, *27*(1), 35-39.

Elser, J. J., M. E. S. Bracken, E. E. Cleland, D. S. Gruner, W. S. Harpole, H. Hillebrand, J. T. Ngai, E. W. Seabloom, J. B. Shurin, and J. E. Smith (2007), Global analysis of nitrogen and phosphorus limitation of primary producers in freshwater, marine and terrestrial ecosystems, *Ecology letters*, *10*(12), 1135-1142.

FÖHse, D., N. Claassen, and A. Jungk (1988), Phosphorus efficiency of plants: I. External and internal P requirement and P uptake efficiency of different plant species, *Plant and Soil*, 101-109.

Friedlingstein, P., P. Cox, R. Betts, L. Bopp, W. Von Bloh, V. Brovkin, P. Cadule, S. Doney, M. Eby, and I. Fung (2006), Climate-carbon cycle feedback analysis: Results from the C4MIP model intercomparison, *Journal of Climate*, *19*(14), 3337-3353.

Hobbie, J. E., and E. A. Hobbie (2006), 15N in symbiotic fungi and plants estimates nitrogen and carbon flux rates in arctic tundra, *Ecology*, *87*(4), 816-822.

Hodge, A., and A. H. Fitter (2010), Substantial nitrogen acquisition by arbuscular mycorrhizal fungi from organic material has implications for N cycling, *Proceedings of the National Academy of Sciences*, *107*(31), 13754-13759.

Hodge, A., D. Robinson, and A. Fitter (2000a), Are microorganisms more effective than plants at competing for nitrogen?, *Trends in plant science*, *5*(7), 304-308.

Hodge, A., J. Stewart, D. Robinson, B. S. Griffiths, and A. H. Fitter (2000b), Competition between roots and soil micro‐organisms for nutrients from nitrogen‐rich patches of varying complexity, *Journal of Ecology*, *88*(1), 150-164.

835 Houghton, R. A. (2003), Revised estimates of the annual net flux of carbon to the
836 atmosphere from changes in land use and land management 1850–2000,
837 *Tellus B*, *55*(2), 378-390.
838 Hu, S., F. S. Chapin, M. K. Firestone, C. B. Field, and N. R. Chiariello (2001), Nitrogen
839 limitation of microbial decomposition in a grassland under elevated CO2,
840 *Nature*, *409*(6817), 188-191.
841 Iversen, C. M., T. D. Hooker, A. T. Classen, and R. J. Norby (2011), Net mineralization
842 of N at deeper soil depths as a potential mechanism for sustained forest
843 production under elevated [CO2], *Global change biology*, *17*(2), 1130-1139.
844 Jackson, R. B., C. W. Cook, J. S. Pippen, and S. M. Palmer (2009), Increased
845 belowground biomass and soil CO2 fluxes after a decade of carbon dioxide
846 enrichment in a warm-temperate forest, *Ecology*, *90*(12), 3352-3366.
847 Jackson, R. B., H. A. Mooney, and E. D. Schulze (1997), A global budget for fine root
848 biomass, surface area, and nutrient contents, *Proceedings of the National*
849 *Academy of Sciences*, *94*(14), 7362-7366.
850 Ji, D., et al. (2014), Description and basic evaluation of Beijing Normal University
851 Earth System Model (BNU-ESM) version 1, *Geosci. Model Dev.*, *7*(5), 2039-
852 2064, doi:10.5194/gmd-7-2039-2014.
853 Johnson, D. W. (1992), Nitrogen retention in forest soils, *Journal of Environmental*
854 *Quality*, *21*(1), 1-12.
855 Kaspari, M., M. N. Garcia, K. E. Harms, M. Santana, S. J. Wright, and J. B. Yavitt (2008),
856 Multiple nutrients limit litterfall and decomposition in a tropical forest,
857 *Ecology Letters*, *11*(1), 35-43.

858 Kaye, J. P., and S. C. Hart (1997), Competition for nitrogen between plants and soil
859 microorganisms, *Trends in Ecology & Evolution*, *12*(4), 139-143.
860 Korsaeth, A., L. Molstad, and L. R. Bakken (2001), Modelling the competition for
861 nitrogen between plants and microflora as a function of soil heterogeneity,
862 *Soil Biology and Biochemistry*, *33*(2), 215-226.
863 Koven, C. D., W. J. Riley, Z. M. Subin, J. Y. Tang, M. S. Torn, W. D. Collins, G. B. Bonan, D.
864 M. Lawrence, and S. C. Swenson (2013), The effect of vertically resolved soil
865 biogeochemistry and alternate soil C and N models on C dynamics of CLM4,
866 *Biogeosciences*, *10*, 7109-7131.
867 Kuzyakov, Y., and X. Xu (2013), Competition between roots and microorganisms for
868 nitrogen: mechanisms and ecological relevance, *New Phytologist*, *198*(3),
869 656-669.
870 Lambers, H., C. Mougel, B. Jaillard, and P. Hinsinger (2009), Plant-microbe-soil
871 interactions in the rhizosphere: an evolutionary perspective, *Plant and Soil*,
872 *321*(1-2), 83-115.
873 Le Quéré, C., R. J. Andres, T. Boden, T. Conway, R. A. Houghton, J. I. House, G. Marland,
874 G. P. Peters, G. R. van der Werf, and A. Ahlström (2013), The global carbon
875 budget 1959–2011, *Earth System Science Data*, *5*(1), 165-185.
876 Le Quéré, C., M. R. Raupach, J. G. Canadell, and G. Marland (2009), Trends in the
877 sources and sinks of carbon dioxide, *Nature Geoscience*, *2*(12), 831-836.
878 LeBauer, D. S., and K. K. Treseder (2008), Nitrogen limitation of net primary
879 productivity in terrestrial ecosystems is globally distributed, *Ecology*, *89*(2),
880 371-379.

881 Li, C., J. Aber, F. Stange, K. Butterbach‐Bahl, and H. Papen (2000), A process‐
882 oriented model of N2O and NO emissions from forest soils: 1. Model
883 development, *Journal of Geophysical Research: Atmospheres (1984–2012)*,
884 *105*(D4), 4369-4384.
885 Maggi, F., C. Gu, W. J. Riley, G. M. Hornberger, R. T. Venterea, T. Xu, N. Spycher, C.
886 Steefel, N. L. Miller, and C. M. Oldenburg (2008), A mechanistic treatment of
887 the dominant soil nitrogen cycling processes: Model development, testing,
888 and application, *Journal of Geophysical Research: Biogeosciences (2005–2012)*,
889 *113*(G2).
890 Maggi, F., and W. J. Riley (2009), Transient competitive complexation in biological
891 kinetic isotope fractionation explains nonsteady isotopic effects: Theory and
892 application to denitrification in soils, *Journal of Geophysical Research:*
893 *Biogeosciences (2005–2012)*, *114*(G4).
894 Marion, G. M., P. C. Miller, J. Kummerow, and W. C. Oechel (1982), Competition for
895 nitrogen in a tussock tundra ecosystem, *Plant and soil*, *66*(3), 317-327.
896 Marland, G., T. A. Boden, R. J. Andres, A. L. Brenkert, and C. A. Johnston (2003),
897 Global, regional, and national fossil fuel CO2 emissions, *Trends: A*
898 *compendium of data on global change*, 34-43.
899 Matson, P., K. A. Lohse, and S. J. Hall (2002), The globalization of nitrogen
900 deposition: consequences for terrestrial ecosystems, *AMBIO: A Journal of the*
901 *Human Environment*, *31*(2), 113-119.

902 Matson, P., W. H. McDowell, A. R. Townsend, and P. M. Vitousek (1999), The
903 globalization of N deposition: ecosystem consequences in tropical
904 environments, *Biogeochemistry*, *46*(1-3), 67-83.
905 McGroddy, M. E., W. L. Silver, R. C. De Oliveira, W. Z. De Mello, and M. Keller (2008),
906 Retention of phosphorus in highly weathered soils under a lowland
907 Amazonian forest ecosystem, *Journal of Geophysical Research: Biogeosciences*
908 *(2005–2012)*, *113*(G4).
909 McGuire, A. D., J. M. Melillo, L. A. Joyce, D. W. Kicklighter, A. L. Grace, B. Moore, and C.
910 J. Vorosmarty (1992), Interactions between carbon and nitrogen dynamics in
911 estimating net primary productivity for potential vegetation in North
912 America, *Global Biogeochemical Cycles*, *6*(2), 101-124.
913 Medvigy, D., S. C. Wofsy, J. W. Munger, D. Y. Hollinger, and P. R. Moorcroft (2009),
914 Mechanistic scaling of ecosystem function and dynamics in space and time:
915 Ecosystem Demography model version 2, *Journal of Geophysical Research:*
916 *Biogeosciences (2005–2012)*, *114*(G1).
917 Min, X., M. Y. Siddiqi, R. D. Guy, A. D. M. Glass, and H. J. Kronzucker (2000), A
918 comparative kinetic analysis of nitrate and ammonium influx in two early‐
919 successional tree species of temperate and boreal forest ecosystems, *Plant,*
920 *Cell & Environment*, *23*(3), 321-328.
921 Moorcroft, P. R., G. C. Hurtt, and S. W. Pacala (2001), A method for scaling vegetation
922 dynamics: the ecosystem demography model (ED), *Ecological monographs*,
923 *71*(4), 557-586.

924 Moorhead, D. L., and R. L. Sinsabaugh (2006), A theoretical model of litter decay and
925 microbial interaction, *Ecological Monographs*, *76*(2), 151-174.
926 Mooshammer, M., W. Wanek, S. Zechmeister-Boltenstern, and A. Richter (2014),
927 Stoichiometric imbalances between terrestrial decomposer communities and
928 their resources: mechanisms and implications of microbial adaptations to
929 their resources, *Frontiers in microbiology*, *5*.
930 Murray, R. E., L. L. Parsons, and M. S. Smith (1989), Kinetics of nitrate utilization by
931 mixed populations of denitrifying bacteria, *Applied and Environmental*
932 *Microbiology*, *55*(3), 717-721.
933 Nedwell, D. B. (1999), Effect of low temperature on microbial growth: lowered
934 affinity for substrates limits growth at low temperature, *FEMS Microbiology*
935 *Ecology*, *30*(2), 101-111.
936 Norby, R. J., J. Ledford, C. D. Reilly, N. E. Miller, and E. G. O'Neill (2004), Fine-root
937 production dominates response of a deciduous forest to atmospheric CO2
938 enrichment, *Proceedings of the National Academy of Sciences of the United*
939 *States of America*, *101*(26), 9689-9693.
940 Norby, R. J., J. M. Warren, C. M. Iversen, B. E. Medlyn, and R. E. McMurtrie (2010),
941 CO2 enhancement of forest productivity constrained by limited nitrogen
942 availability, *Proceedings of the National Academy of Sciences*, *107*(45), 19368-
943 19373.
944 Nordin, A., P. Högberg, and T. Näsholm (2001), Soil nitrogen form and plant nitrogen
945 uptake along a boreal forest productivity gradient, *Oecologia*, *129*(1), 125-
946 132.

947 Olander, L. P., and P. M. Vitousek (2004), Biological and geochemical sinks for
948 phosphorus in soil from a wet tropical forest, *Ecosystems*, *7*(4), 404-419.
949 Olander, L. P., and P. M. Vitousek (2005), Short-term controls over inorganic
950 phosphorus during soil and ecosystem development, *Soil Biology and*
951 *Biochemistry*, *37*(4), 651-659.
952 Oren, R., D. S. Ellsworth, K. H. Johnsen, N. Phillips, B. E. Ewers, C. Maier, K. V. R.
953 Schäfer, H. McCarthy, G. Hendrey, and S. G. McNulty (2001), Soil fertility
954 limits carbon sequestration by forest ecosystems in a CO2-enriched
955 atmosphere, *Nature*, *411*(6836), 469-472.
956 Pappas, C., S. Fatichi, S. Leuzinger, A. Wolf, and P. Burlando (2013), Sensitivity
957 analysis of a process‐based ecosystem model: Pinpointing parameterization
958 and structural issues, *Journal of Geophysical Research: Biogeosciences*, *118*(2),
959 505-528.
960 Parton, W. J., E. A. Holland, S. J. Del Grosso, M. D. Hartman, R. E. Martin, A. R. Mosier,
961 D. S. Ojima, and D. S. Schimel (2001), Generalized model for NO x and N2O
962 emissions from soils, *Journal of Geophysical Research: Atmospheres (1984–*
963 *2012)*, *106*(D15), 17403-17419.
964 Parton, W. J., J. W. B. Stewart, and C. V. Cole (1988), Dynamics of C, N, P and S in
965 grassland soils: a model, *Biogeochemistry*, *5*(1), 109-131.
966 Perakis, S. S., and L. O. Hedin (2002), Nitrogen loss from unpolluted South American
967 forests mainly via dissolved organic compounds, *Nature*, *415*(6870), 416-
968 419.

969 Phillips, R. P., A. C. Finzi, and E. S. Bernhardt (2011), Enhanced root exudation
970 induces microbial feedbacks to N cycling in a pine forest under long‐term
971 CO2 fumigation, *Ecology Letters*, *14*(2), 187-194.
972 Potter, C. S., J. T. Randerson, C. B. Field, P. A. Matson, P. M. Vitousek, H. A. Mooney,
973 and S. A. Klooster (1993), Terrestrial ecosystem production: a process model
974 based on global satellite and surface data, *Global Biogeochemical Cycles*, *7*(4),
975 811-841.
976 Provides, G. F. W. I. (2014), Climate Model Intercomparisons: Preparing for the Next
977 Phase, *Eos*, *95*(9).
978 Raynaud, X., J.-C. Lata, and P. W. Leadley (2006), Soil microbial loop and nutrient
979 uptake by plants: a test using a coupled C: N model of plant–microbial
980 interactions, *Plant and Soil*, *287*(1-2), 95-116.
981 Raynaud, X., and P. W. Leadley (2004), Soil characteristics play a key role in
982 modeling nutrient competition in plant communities, *Ecology*, *85*(8), 2200-
983 2214.
984 Reich, P. B., and S. E. Hobbie (2013), Decade-long soil nitrogen constraint on the CO2
985 fertilization of plant biomass, *Nature Climate Change*, *3*(3), 278-282.
986 Reich, P. B., S. E. Hobbie, T. Lee, D. S. Ellsworth, J. B. West, D. Tilman, J. M. H. Knops, S.
987 Naeem, and J. Trost (2006), Nitrogen limitation constrains sustainability of
988 ecosystem response to CO2, *Nature*, *440*(7086), 922-925.
989 Reynolds, H. L., and S. W. Pacala (1993), An analytical treatment of root-to-shoot
990 ratio and plant competition for soil nutrient and light, *American Naturalist*,
991 51-70.

992 Ricciuto, D. M., K. J. Davis, and K. Keller (2008), A Bayesian calibration of a simple
993 carbon cycle model: The role of observations in estimating and reducing
994 uncertainty, *Global biogeochemical cycles*, *22*(2).
995 Rillig, M. C., M. F. Allen, J. N. Klironomos, N. R. Chiariello, and C. B. Field (1998), Plant
996 species-specific changes in root-inhabiting fungi in a California annual
997 grassland: responses to elevated CO2 and nutrients, *Oecologia*, *113*(2), 252-
998 259.
999 Running, S. W., and J. C. Coughlan (1988), A general model of forest ecosystem
1000 processes for regional applications I. Hydrologic balance, canopy gas
1001 exchange and primary production processes, *Ecological modelling*, *42*(2),
1002 125-154.
1003 Schimel, J. P., and J. Bennett (2004), Nitrogen mineralization: challenges of a
1004 changing paradigm, *Ecology*, *85*(3), 591-602.
1005 Schimel, J. P., L. E. Jackson, and M. K. Firestone (1989), Spatial and temporal effects
1006 on plant-microbial competition for inorganic nitrogen in a California annual
1007 grassland, *Soil Biology and Biochemistry*, *21*(8), 1059-1066.
1008 Scholze, M., T. Kaminski, P. Rayner, W. Knorr, and R. Giering (2007), Propagating
1009 uncertainty through prognostic carbon cycle data assimilation system
1010 simulations, *Journal of Geophysical Research: Atmospheres (1984–2012)*,
1011 *112*(D17).
1012 Shen, J., L. Yuan, J. Zhang, H. Li, Z. Bai, X. Chen, W. Zhang, and F. Zhang (2011),
1013 Phosphorus dynamics: from soil to plant, *Plant physiology*, *156*(3), 997-1005.

1014 Silver, W. L., A. W. Thompson, M. E. McGroddy, R. K. Varner, J. R. Robertson, H. S. J.D.
1015 Dias, P. Crill, and M. Keller (2012), LBA-ECO TG-07 Long-Term Soil Gas Flux
1016 and Root Mortality, Tapajos National Forest. Data set. Available on-line
1017 [http://daac.ornl.gov] from Oak Ridge National Laboratory Distributed
1018 Active Archive Center, *Oak Ridge, Tennessee, U.S.A.*,
1019 http://dx.doi.org/10.3334/ORNLDAAC/1116.
1020 Sokolov, A. P., D. W. Kicklighter, J. M. Melillo, B. S. Felzer, C. A. Schlosser, and T. W.
1021 Cronin (2008), Consequences of considering carbon-nitrogen interactions on
1022 the feedbacks between climate and the terrestrial carbon cycle, *Journal of*
1023 *Climate*, *21*(15), 3776-3796.
1024 Springate, D. A., and P. X. Kover (2014), Plant responses to elevated temperatures: a
1025 field study on phenological sensitivity and fitness responses to simulated
1026 climate warming, *Global change biology*, *20*(2), 456-465.
1027 Stocker, T. F., D. Qin, G.-K. Plattner, M. Tignor, S. K. Allen, J. Boschung, A. Nauels, Y.
1028 Xia, V. Bex, and P. M. Midgley (2013), Climate Change 2013. The Physical
1029 Science Basis. Working Group I Contribution to the Fifth Assessment Report
1030 of the Intergovernmental Panel on Climate Change-Abstract for decision-
1031 makers*Rep.*, Groupe d'experts intergouvernemental sur l'evolution du
1032 climat/Intergovernmental Panel on Climate Change-IPCC, C/O World
1033 Meteorological Organization, 7bis Avenue de la Paix, CP 2300 CH-1211
1034 Geneva 2 (Switzerland).
1035 Tang, J. Y., and W. J. Riley (2013), A total quasi-steady-state formulation of substrate
1036 uptake kinetics in complex networks and an example application to microbial

litter decomposition, *Biogeosciences*, *10*(12), 8329-8351, doi:10.5194/bg-10-8329-2013.

Tang, J. Y., and W. J. Riley (2014), Weaker soil carbon-climate feedbacks resulting from microbial and abiotic interactions, *Nature Clim. Change*, *advance online publication*, doi:10.1038/nclimate2438 http://www.nature.com/nclimate/journal/vaop/ncurrent/abs/nclimate2438.html - supplementary-information.

Templer, P. H., W. L. Silver, J. Pett-Ridge, K. M. DeAngelis, and M. K. Firestone (2008), Plant and microbial controls on nitrogen retention and loss in a humid tropical forest, *Ecology*, *89*(11), 3030-3040.

Thomas, R. Q., G. B. Bonan, and C. L. Goodale (2013a), Insights into mechanisms governing forest carbon response to nitrogen deposition: a model-data comparison using observed responses to nitrogen addition, *Biogeosciences Discussions*, *10*(1), 1635-1683.

Thomas, R. Q., S. Zaehle, P. H. Templer, and C. L. Goodale (2013b), Global patterns of nitrogen limitation: confronting two global biogeochemical models with observations, *Global change biology*, *19*(10), 2986-2998.

Thornton, P. E., J. F. Lamarque, N. A. Rosenbloom, and N. M. Mahowald (2007), Influence of carbon‐nitrogen cycle coupling on land model response to CO2 fertilization and climate variability, *Global Biogeochemical Cycles*, *21*(4).

Treseder, K. K., and P. M. Vitousek (2001), Effects of soil nutrient availability on investment in acquisition of N and P in Hawaiian rain forests, *Ecology*, *82*(4), 946-954.

1060 Trumbore, S., E. S. Da Costa, D. C. Nepstad, P. Barbosa De Camargo, L. A. Martinelli, D.
1061 Ray, T. Restom, and W. Silver (2006), Dynamics of fine root carbon in
1062 Amazonian tropical ecosystems and the contribution of roots to soil
1063 respiration, *Global Change Biology*, *12*(2), 217-229.
1064 Vitousek, P. M., and H. Farrington (1997), Nutrient limitation and soil development:
1065 experimental test of a biogeochemical theory, *Biogeochemistry*, *37*(1), 63-75.
1066 Vitousek, P. M., and R. W. Howarth (1991), Nitrogen limitation on land and in the
1067 sea: how can it occur?, *Biogeochemistry*, *13*(2), 87-115.
1068 Vitousek, P. M., S. Porder, B. Z. Houlton, and O. A. Chadwick (2010), Terrestrial
1069 phosphorus limitation: mechanisms, implications, and nitrogen-phosphorus
1070 interactions, *Ecological applications*, *20*(1), 5-15.
1071 Vitousek, P. M., and R. L. Sanford (1986), Nutrient cycling in moist tropical forest,
1072 *Annual review of Ecology and Systematics*, 137-167.
1073 Waksman, S. A. (1931), Principles of soil microbiology, *Principles of soil*
1074 *microbiology.*
1075 Walker, T. W., and J. K. Syers (1976), The fate of phosphorus during pedogenesis,
1076 *Geoderma*, *15*(1), 1-19.
1077 Wang, J., and B. Lars, R (1997), Competition for nitrogen during mineralization of
1078 plant residues in soil: microbial response to C and N availability, *Soil Biology*
1079 *and Biochemistry*, *29*(2), 163-170.
1080 Wang, Y. P., B. Z. Houlton, and C. B. Field (2007), A model of biogeochemical cycles of
1081 carbon, nitrogen, and phosphorus including symbiotic nitrogen fixation and
1082 phosphatase production, *Global Biogeochemical Cycles*, *21*(1).

1083 Wang, Y. P., R. M. Law, and B. Pak (2010), A global model of carbon, nitrogen and
1084 phosphorus cycles for the terrestrial biosphere, *Biogeosciences*, *7*(7), 2261-
1085 2282.
1086 Wieder, W. R., C. C. Cleveland, and A. R. Townsend (2009), Controls over leaf litter
1087 decomposition in wet tropical forests, *Ecology*, *90*(12), 3333-3341.
1088 Woodmansee, R. G., I. Vallis, and J. J. Mott (1981), Grassland nitrogen, *Ecological*
1089 *Bulletins (Sweden)*.
1090 Xu, X., P. E. Thornton, and W. M. Post (2013), A global analysis of soil microbial
1091 biomass carbon, nitrogen and phosphorus in terrestrial ecosystems, *Global*
1092 *Ecology and Biogeography*, *22*(6), 737-749.
1093 Yang, X., P. E. Thornton, D. M. Ricciuto, and W. M. Post (2014), The role of
1094 phosphorus dynamics in tropical forests–a modeling study using CLM-CNP,
1095 *Biogeosciences*, *11*(6), 1667-1681.
1096 Zaehle, S., and D. Dalmonech (2011), Carbon–nitrogen interactions on land at global
1097 scales: current understanding in modelling climate biosphere feedbacks,
1098 *Current Opinion in Environmental Sustainability*, *3*(5), 311-320.
1099 Zaehle, S., P. Friedlingstein, and A. D. Friend (2010), Terrestrial nitrogen feedbacks
1100 may accelerate future climate change, *Geophysical Research Letters*, *37*(1).
1101 Zaehle, S., and A. D. Friend (2010), Carbon and nitrogen cycle dynamics in the O‐
1102 CN land surface model: 1. Model description, site‐scale evaluation, and
1103 sensitivity to parameter estimates, *Global Biogeochemical Cycles*, *24*(1).
1104 Zaehle, S., B. E. Medlyn, M. G. De Kauwe, A. P. Walker, M. C. Dietze, T. Hickler, Y. Luo,
1105 Y. P. Wang, B. El‐Masri, and P. Thornton (2014), Evaluation of 11 terrestrial

carbon‐nitrogen cycle models against observations from two temperate Free‐Air CO2 Enrichment studies, *New Phytologist*, *202*(3), 803-822.

Zhang, Q., Y. P. Wang, A. J. Pitman, and Y. J. Dai (2011), Limitations of nitrogen and phosphorous on the terrestrial carbon uptake in the 20th century, *Geophysical Research Letters*, *38*(22).

Zhu, Q., and W. J. Riley (2015), Improved modelling of soil nitrogen losses, *Nature Climate Change*, *5*(8), 705-706.

Zhu, Q., and Q. Zhuang (2013), Modeling the effects of organic nitrogen uptake by plants on the carbon cycling of boreal ecosystems, *Biogeosciences*, *10*(8), 13455-13490.

Zhu, Q., and Q. Zhuang (2014), Parameterization and sensitivity analysis of a process‐based terrestrial ecosystem model using adjoint method, *Journal of Advances in Modeling Earth Systems*.